

On the coupling between precipitation and potential evapotranspiration: contributions to decadal drought anomalies in the Southwest China

Shanlei Sun^{1,2} · Haishan Chen¹ · Weimin Ju³ · Guojie Wang⁴ · Ge Sun⁵ · Jin Huang⁶ · Hedi Ma¹ · Chujie Gao¹ · Wenjian Hua¹ · Guixia Yan²

Received: 14 October 2015 / Accepted: 28 July 2016 / Published online: 6 August 2016
© Springer-Verlag Berlin Heidelberg 2016

Abstract Under the exacerbation of climate change, climate extreme events, especially for drought, happened frequently and intensively across the globe with greater spatial differences. We used the Standardized Precipitation-Evapotranspiration Index computed from the routine meteorological observations at 269 sites in Southwest China (SWC) to study the drought characteristics (e.g., extent, duration and intensity) and their decadal variations during 1971–2012. It was revealed that the drought, in responses to the coupling between decadal precipitation and potential evapotranspiration (PET) anomalies, differed among regions and periods. For the entire SWC, droughts in 1970s and 2000s+ was generally stronger than in 1980s and 1990s with respect

to their spatial extent, duration and intensity, especially in 2000s+. It was well-known that drought was closely related with a lack of precipitation; however, the impact of atmospheric demand of evaporation (reflected by PET here) on drought (e.g., duration and intensity) was rarely paid enough attentions. To that end, a spatial multi-linear regression approach was proposed in this study for quantifying the contributions of decadal PET and precipitation variations to drought duration and intensity. We have found that the contributions of decadal PET anomalies to drought duration and intensity could exceed those of precipitation, e.g., during 1980s and 1990s in SWC. Additionally, despite the strongest droughts in 2000s+, it was suggested that PET could exert comparable impacts on drought anomalies as precipitation. All these findings implied that PET plays a critical role in drought event, which acts to amplify drought duration and intensity. To sum up, this study stressed the need for enough attentions for PET processes in drought studies.

Electronic supplementary material The online version of this article (doi:10.1007/s00382-016-3302-5) contains supplementary material, which is available to authorized users.

✉ Haishan Chen
haishan@nuist.edu.cn

¹ Collaborative Innovation Center on Forecast and Evaluation of Meteorological Disasters/Key Laboratory of Meteorological Disaster, Ministry of Education/International Joint Research Laboratory on Climate and Environment Change, Nanjing University of Information Science and Technology (NUIST), Nanjing, China

² Applied Hydrometeorological Research Institute, NUIST, Nanjing, China

³ International Institute for Earth System Science (ESSI), Nanjing University, Nanjing, China

⁴ School of Geography and Remote Sensing, NUIST, Nanjing, China

⁵ United States Department of Agriculture Forest Services, Eastern Forest Environmental Threat Assessment Center, Southern Research Station, Raleigh, NC, USA

⁶ School of Applied Meteorology, NUIST, Nanjing, China

Keywords Drought · Potential evapotranspiration · Decadal anomaly · SPEI · Southwest China

1 Introduction

The Fifth Assessment Report of the Intergovernmental Panel on Climate Change has pointed out that Global Mean Surface Temperature (GMST) has increased the instrumental records during the last 100 years especially in since 1960s; and, the first decade of the twenty-first century has become the warmest (IPCC 2014). With the successive and rapid warming during the past decades, more and more evidences have suggested that climate extremes (e.g., extreme precipitation, heatwave, tropical cyclones and droughts) at

both regional and global scales, are increasing with different confidence levels (Stott et al. 2004; Elsner et al. 2008; Min et al. 2011; Sheffield et al. 2012; Dai et al. 2004; Dai 2013; Trenberth et al. 2012; IPCC 2014). Among all the extremes, droughts are believed to be the most damaging natural disasters [Federal Emergency Management Agency (FEMA), 1995; Romm 2011], which affects more people than any other forms of devastating meteorological hazards (Wilhite 2000; Yu et al. 2014) and causes global damages of billions dollars. For example, droughts have cost more than \$144 billion for the United States from 1980 to 2003 (Li et al. 2013); meanwhile, an intense and prolonged drought of China during 2009/2010 caused total economic losses of at least \$3.5 billion (Barriopedro et al. 2012). Consequently, numerous studies have focused on the drought variations and its adverse impacts in the background of changing and even exacerbating climate on both global and regional scales (Palmer 1965; Mckee et al. 1993; Wells et al. 2004; Vicente-Serrano et al. 2010; Vergni and Todisco 2011; Sheffield et al. 2012; Choi et al. 2013; Dai 2011, 2013; Kogan et al. 2013; Li et al. 2013; Trenberth et al. 2012; Zhang and Jia 2013; Qin et al. 2015b). For example, Dai (2013) stated that drought would increase under the global warming based on instrumental observations and numerical simulations. However, Trenberth et al. (2012) compared the apparently conflicting results of Dai (2013) and Sheffield et al. (2012) on drought changes with climate change, and suggested that droughts were likely to be quicker and more intense despite the lower occurrence probability induced by global warming.

China is frequently stricken by natural disasters, in particular drought. During the second half of twentieth century, China has suffered from long-lasting and severe droughts, consequently resulting in devastating economic and social losses [National Climate Center (NCC) 1998; Huang et al. 2006; Qian et al. 2011; Lü et al. 2012; Yang et al. 2013; Yu et al. 2014]. For instance, Yu et al. (2014) found that severe and extreme droughts have become more serious since late 1990s throughout China (with an increase of dry area by ~3.72 % per decade) based on Standardized Precipitation-Evapotranspiration Index (SPEI). Yang et al. (2013) identified severe droughts in China during 1961–2010 with the Multi-Scale Standardized Precipitation Index (MSPI), and stated that the severe droughts have presented a trend of gradual increase especially in autumn. Nevertheless, changes in drought and the related mechanisms within China are different from region to region, due to different regional effects of climate changes (Wang et al. 2013a, b). Since the start of twenty-first century, a significant increase in extreme drought has been observed in Southwest China (SWC) (Duan et al. 2000; Hu et al. 2009; Huang 2011; Barriopedro et al. 2012; Feng et al. 2014; Zhang et al. 2012a, b, 2013, 2014; Wang et al. 2015a, b,

2016; Xu et al. 2015a). Particularly, several provinces [i.e., Sichuan (SC), Chongqing (CQ), Guizhou (GZ), Yunnan (YN) and Guangxi (GX)] within SWC have experienced sustained and severe droughts during 2006 and 2009/2010, which has constituted devastating and far-reaching threats to agriculture, water availability and ecosystems (Qiu, 2010; Barriopedro et al. 2012; Ye et al. 2012; Zhang et al. 2012a, b; Wang and Chen 2014; Qin et al. 2015a). Notably, Yang et al. (2012a) has pointed out that this drought occurred in SWC was the most severe drought during the last five decades, and thus could be believed to be a ‘once-in-a-century’ drought, which was reported that more than 60 million residents suffered from drinking-water shortages, and crops of more than 1 million had died (Zhang et al. 2013). For studying the mechanisms of this drought and the likewise ones, more and more efforts have been devoted to precipitation deficiency from the perspective of atmospheric dynamic, including El Niño-Southern Oscillation (ENSO) and North Atlantic Oscillation (NAO) (Li et al. 2009; Barriopedro et al. 2012; Qian and Zhang 2012; Zhang et al. 2013, 2014; Feng et al. 2014; Wang et al. 2015b). Zhang et al. (2013) revealed that the strong autumn drought over SWC in 2009 was predominantly attributed to the concurrent distinctive warm pool El Niño, which generated a strongly anomalous cyclone over the west North Pacific, and consequently induced a serious decrease in rainfall over this region. Based on the measured rainfall and reanalysis data, Feng et al. (2014) found that the severe SWC droughts during 1951–2010 were closely related to the circulation anomalies caused by remote forcing from the tropical Pacific and North Atlantic Oceans.

To sum up, numerous studies have carried out relatively thorough analyses of SWC droughts, and reached general agreement that drought in SWC has become more frequent and intense during the last five decades in observations and projections (Wang and Chen 2014; Wang et al. 2015a). Nevertheless, it is worth noting that most of these researches only emphasized precipitation for explaining and predicting drought variations, but scarcely considered the impact of atmospheric evaporative demand which can be reflected by potential evapotranspiration (PET). Seen from the concept of soil water balance, PET plays a major role in influencing soil water loss (Monteith 1973, 1976; Abramopoulos et al. 1988; Hobbins et al. 2008). As a result, lacking considerations of PET impact may introduce uncertainties into drought analyses and the possible mechanisms as well as the accurate forecast practice. Recently, some scholars have warned against systematically ignoring the importance of PET influences in drought conditions (Hu and Willson 2000; Vicente-Serrano et al. 2010, 2015; Wang and Chen 2012; Teuling et al. 2013; Wang et al. 2014a; Xu et al. 2015b). For example, Hu and Willson (2000) stated that drought responses to precipitation and temperature

(used for calculating PET) were of the same order. Briefly, for better understanding the physical mechanisms of drought variations, and improving its monitoring and predicting, it is crucial to consider PET impacts on drought and to determine how and what magnitudes the on-going changes in PET and precipitation have influenced drought. Up to date, however, there remains a challenge in quantifying the respective impact of these two factors due to their complicated interactions. Therefore, the present study aims to: (1) comprehensively evaluate decadal drought anomalies (e.g., extent, duration and intensity) during 1971–2012 based on 3-month SPEI, which were estimated using observations from 269 weather sites observations in SWC; and (2) quantify the individual contributions of precipitation and PET to decadal anomalies of drought duration and intensity based on a spatial multi-linear regression model.

In the remainder of this study, Sect. 2 described the study region, the used datasets and methodology. Section 3 illustrated the climatologic precipitation, PET and drought characteristics during 1971–2012, their decadal anomalies, and contributions of decadal precipitation and PET anomalies to drought duration and intensity. Possible causes of decadal precipitation and PET anomalies, and some uncertainties of this study were discussed in Sect. 4. Finally, the major findings were summarized in Sect. 5.

2 Data and methodology

2.1 Study area and data

In this current study, SWC is specified between 21–34°N and 97–110°E, and encompasses a large geographic area ranging from the high plateau of west SC and YN to the low-lying SC basin, which mainly includes SC, CQ, GZ and YN province, and west part of GX province (wGX; Fig. 1). As one of the most densely populated area, it accounts for about 1/6 of the total population of China. It is also a main grain producing area, providing approximately 16 % of the national food supply. Across SWC, a typical subtropical monsoon climate prevails with clearly defined dry/wet season, and rainy season usually beginning in April and ending in October.

To drive SPEI model, the routine meteorological observations were required. Here, monthly precipitation (P ; mm/month), maximum and minimum temperature (°C), relative humidity (%), sunshine duration (h/month) and wind speed at 10 (m/s) measured during 1969–2012 at 334 weather sites were collected from China Meteorological Administration (CMA). Note that two data quality issues for the historical meteorological observations needed to be mentioned here: (1) Inhomogeneity. For the long-term meteorological datasets, Wijngaard et al. (2003) stated that

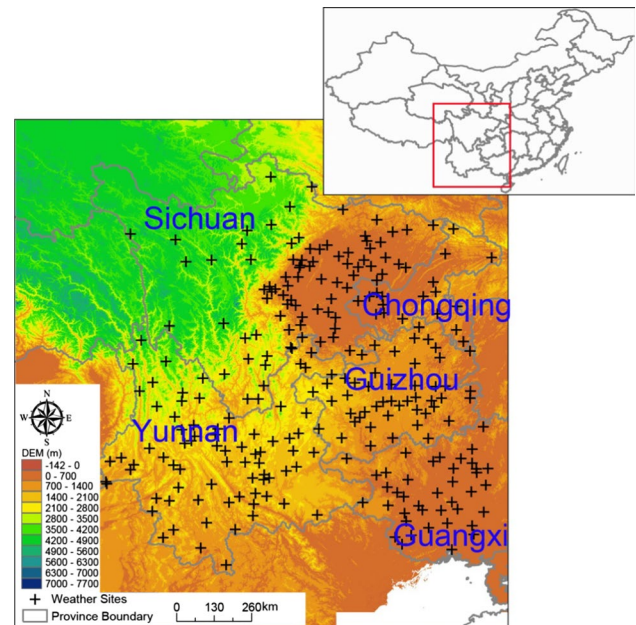


Fig. 1 Location of SWC with 269 weather sites. The shading denotes the elevation, which is represented using digital elevation model (DEM) with the spatial resolution of 90 m \times 90 m. This data can be obtained from <http://srtm.csi.cgiar.org/>

data inhomogeneity, if not accounted for properly, could largely impact the robustness of study results. Unfortunately, due to a lack of the information about station history metadata, we could not adjust the data homogeneity. Alternatively, *Pettitt* test, a method to test time series homogeneity (Wijngaard et al. 2003), was employed here to check these variables. Each variable at most of stations could pass the significant test at the 5 % level. (2) Missing values. Despite some data gaps, at least more than 10 months had available data in every year. The missing values were filled based on the data from nearby sites using linear regression equations. Lastly, 269 sites were chosen in SWC (Fig. 1).

2.2 Methodology

2.2.1 SPEI model

Wang and Chen (2012) have testified SPEI model in SWC comparing against droughts statistics from yearbooks, and found that SPEI could well reproduce the basic features of droughts. Therefore, SPEI model was selected for obtaining drought characteristics in the current study, which could be operated as follows:

- (1) Previous researches have pointed out that the Thornthwaite equation (Thornthwaite 1948) underestimated PET in arid and semiarid regions (Jensen et al. 1990)

and overestimated PET in humid equatorial and tropical regions (van der Schrier et al. 2011). Additionally, this formulation resulted in an overestimation of PET with increasing air temperature, and did not accurately calculate PET evolution over the last decades (Donohue et al. 2010). Therefore, we computed PET using a modified Penman–Monteith equation (Allen et al. 1998). This equation has been recommended as a standard tool for calculating PET with climatic data by the International Commission for Irrigation (ICID), the Food and Agriculture Organization (FAO) of the United Nations and the American Society of Civil Engineers (ASCE).

$$PET = \frac{0.408 \cdot \Delta \cdot (R_n - G) + \gamma \cdot \frac{900}{T+273} \cdot U_2 \cdot VPD}{\Delta + \gamma \cdot (1 + 0.34 \cdot U_2)} \quad (1)$$

where R_n [MJ/(m²·d)], named as net radiation at reference crop surface, was difference between incoming net shortwave and outgoing net longwave radiation; G [MJ/(m²·d)] denoted soil heat flux density, which could be ignored at monthly or longer time scales; γ (kPa/°C) was psychrometric constant; Δ (kPa/°C) represented the slope vapor pressure curve; U_2 (m/s) converted from wind speed at 10 m height, was wind speed at a 2 m height; VPD (kPa) denoted vapor pressure deficit, which could be estimated from saturation vapor pressure (e_s) multiplying by [1 minus relative humidity (R_h)]; T (°C) represented mean temperature, and equated to the average of maximum and minimum temperatures. Detailed equations about R_n , γ , Δ , U_2 and e_s could be found in the reference of Allen et al. (1998). It was worth noting that all the computations were performed on monthly scale.

- (2) For representing water surplus or deficit in the analyzed month, a simple measure (precipitation minus PET for i th month, named as D_i) was proposed. After that, D_i was able to be aggregated at various time scales, which was prepared for estimating the SPEI at the corresponding time scale (e.g., 3-, 6-, 12- and 24-month).
- (3) Normalize the water balance based on a log-logistic probability distribution to obtain the SPEI time-series.

Similar to precipitation, the probability distribution of D_i is not normal, therefore, a three-parameter log-logistic distribution was recommended to best fit the twelve time series D_i within a year (Vicente-Serrano et al. 2010). Then, an inverse normal function was used to standardize the probabilities (Abramowitz and Stegun 1965; Vicente-Serrano et al. 2010). In the current study, the computation of the SPEI model was carried out by the R package developed by Vicente-Serrano et al. (2010), which could be downloaded

at site of <http://sac.csic.es/spei/tools.html>. About the detailed procedures of the SPEI model, the reader can read the handling instruction (could be found at site of <https://cran.r-project.org/web/packages/SPEI/SPEI.pdf>).

2.2.2 Identification of drought characteristics

In this study, the 3-month SPEI time-series was calculated using monthly observed precipitation and estimated PET during 1971–2012 at 269 sites of SWC, which were selected for analyzing drought characteristics, mainly including drought extent, duration and intensity. Before indentifying drought characteristics, threshold for judging whether a given month appeared drought or not, was requisite. According to the Classification of Meteorological Drought of China, this threshold for drought was set to < -0.5 . When monthly SPEI at some one month was < -0.5 , we could think that drought occurred in this month, and vice versa. Here, we focused on decadal average drought extent (*DADE*), duration (*DADD*) and intensity (*DADI*) for each province and SWC, and their decadal anomalies relative to the multi-year mean during 1971–2012. For each objective region, *DADE* (characterized by number of sites with drought for each period), *DADD* and *DADI* could be estimated by:

$$\left\{ \begin{array}{l} DADE = \frac{1}{yn} \sum_{i=1}^{yn} \left[\frac{1}{12} \sum_{j=1}^{12} \sum_{k=1}^{sn} x_{i,k,j} \right] \\ DADD = \frac{1}{yn} \sum_{i=1}^{yn} \left[\frac{1}{sn} \sum_{k=1}^{sn} \sum_{j=1}^{12} x_{i,k,j} \right] \\ DADI = \frac{1}{yn} \sum_{i=1}^{yn} \left[\frac{1}{sn} \sum_k \left(\frac{1}{n_{k,i}} \sum_{j=1}^{n_{k,i}} y_{k,i,j} \right) \right] \\ \left\{ \begin{array}{l} x_{k,i,j} = 0 \quad (S_{k,i,j} > -0.5) \\ x_{k,i,j} = 1 \quad (S_{k,i,j} < -0.5) \\ y_{k,i,j} = S_{k,i,j} \quad (S_{k,i,j} < -0.5) \end{array} \right. \end{array} \right. \quad (2)$$

where $S_{k,i,j}$ was the SPEI value at j th month of i th year for k th site. sn represented the number of site within the study region, of which SC, CQ, GZ, YN, wGX and SWC had 84, 18, 49, 77, 41 and 269 sites, respectively; while yn was years for each period with 10 years of 1971–1980 (1970s), 1981–1990 (1980s), 1991–2000 (1990s) and 12 years of 2001–2012 (2000s+). $n_{k,i}$ indicated months with drought at i th year of k th site. For SC, CQ, GZ, YN, wGX and SWC, anomalies of *DADE*, *DADD* and *DADI* were estimated through subtracting 1971–2012 period mean from the corresponding decadal mean. Considering the different spatial spans, furthermore, the percent anomalies of *DADE* were chosen for comparing among all these study regions, which were expressed as anomalies of *DADE* divided by 1971–2012 period mean.

2.2.3 Quantifying contributions of precipitation and PET to DADD and DADI anomalies

Driving factors of drought considered in this study consisted of precipitation and PET, and thus their contributions to *DADD* or *DADI* anomalies were quantified based on a multi-linear regression method. This approach could be described as: (1) For each province or the whole SWC, samples for a multi-linear regression could be integrated as a whole, e.g., the whole SWC including 269 (sites) \times 4 (periods) samples. Then, a multi-linear regression within some one objective region could be established using *DADD* or *DADI* anomalies as dependent variable, and the corresponding decadal precipitation and PET anomalies as independent variables; and (2) Based on the established multi-linear regression coefficients, contributions of decadal precipitation and PET variations to *DADD* or *DADI* anomalies could be calculated. Taking the contributions of decadal precipitation variations to *DADD* as an example, its contribution over the whole SWC was able to be obtained with decadal precipitation variations multiplying by precipitation coefficients from the corresponding regression. Similarly, contributions of decadal precipitation (PET) variations to *DADD* or *DADI* anomalies for each province or the whole SWC could also be calculated using the approach mentioned above. In addition, the potential impacts of spatial differences on results were also considered in this study, through involving the heights and locations (i.e., latitude and longitude) of weather sites into the multi-linear regressions.

It is worth noting that, for matching the time scale of SPEI-3, we have preprocessed precipitation, PET and the other climatic variables (i.e., sunshine duration, mean temperature, VPD and wind speed) by averaging their values in a given month and the previous 2 months. In the following section, if not specified, the analyses were conducted based on the 3-month means.

3 Results

3.1 Climatologic characteristics of precipitation, PET and drought

In soil water balance, precipitation and ET (can be partly reflected by PET) mainly control soil moisture availability, which directly and closely relates to drought; thus, their climatologic characteristics across SWC have been analyzed here. We show first the spatial variations of precipitation and PET derived from 42-year mean values (Fig. 2a, b). In general, precipitation showed gradient decreases from southeast to northwest, of which there were more

than 1000 mm/year for annual precipitation over most sites, especially in south YN and wGX (Fig. 2a). Different from spatial distribution of precipitation, PET basically showed an increase from north to south. Taking the provincial boundaries of YN and wGX as borderline, there was relative higher PET (>1000 mm/year) in south SWC, while that in north SWC was relative lower (<1000 mm/year; Fig. 2b). Figure 3a displayed precipitation and PET averaged over SWC, SC, CQ, GZ, YN and wGX, respectively. Over SWC, annual precipitation and PET were 1118.15 and 971.47 mm/year, respectively (Fig. 3a). The annual precipitation over SC and GZ provinces amounted to around 1000 mm/year; however, that in the other provinces all amounted to more than 1100 mm/year, especially in wGX where it was 1405.56 mm/year. The maximum PET appeared in wGX and YN where it amounted to more than 1100 mm/year; it amounted to around 900 mm/year in all the other provinces.

Due to the complex nature of drought, several drought characteristics, including drought extent, duration and intensity, have been studied for a comprehensive understanding in this current study. Table 1 showed climatologic drought extent across SWC and each province during 1971–2012. It appeared that drought occurred over 87 sites across SWC every year. Despite of greater differences in absolute values of climatologic drought extent due to various spatial span, it was interesting to find that climatologic drought extent divided by number of sites with drought for each region all approximated to 32 %/year, which implied that climatologic characteristics of drought extent in these regions were comparative. Figure 2c, d depicted the spatial distributions of climatologic *DADD* and *DADI* across SWC, respectively. Seen from Fig. 2c, *DADD* exhibited complicate climatologic characters spatially, which ranged from 3.30 to 4.80 month/year. In SC basin, central YN, north GZ and west YN, *DADD* appeared to be greater than 3.90 month/year, which might suggest that drought occurrences often combined with longer duration. For regionally averaged *DADD* within each province, however, there were not obvious differences with fluctuation around 3.80 month/year (Fig. 3b). Similar to the spatial pattern of *DADD*, Fig. 2d illustrated that the climatologic *DADI* had also complex distribution over SWC with regionally averaged mean value of -0.99 (Fig. 3b); and, the *DADI* value of most sites were between -1.10 and -0.96 . Among the five provinces, the regionally averaged *DADI* climatology had similar values around -1.00 (Fig. 3c).

Generally, climatologic precipitation and PET over SWC exhibited relative evident differences in terms of spatial distributions and regional average, possibly due to precipitation mechanisms, PET divers and topography. Just under the allocations of precipitation and PET over SWC,

Fig. 2 Spatial distribution of climatologic precipitation **a**, PET **b**, *DADD* **c** and *DADI* **d** across SWC during 1971–2012

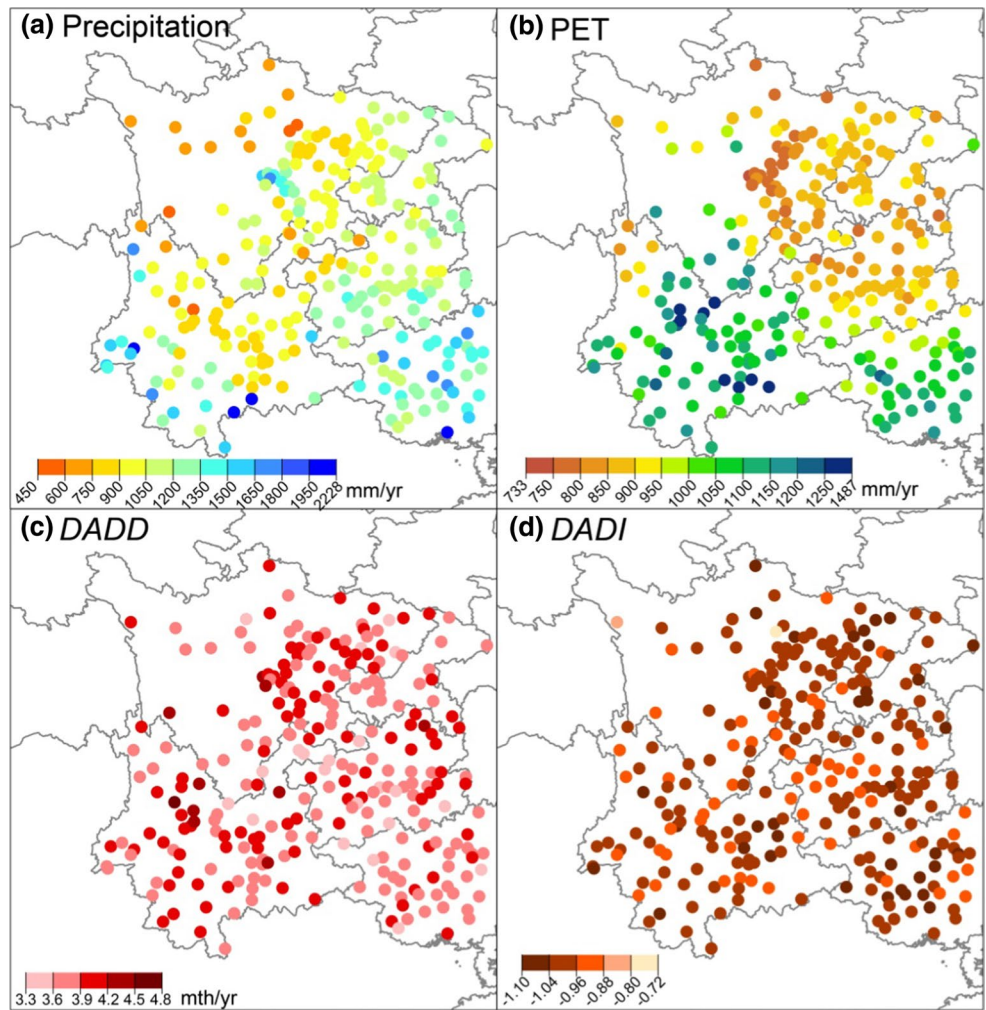


Fig. 3 Climatologic precipitation and PET **(a)**, and *DADD* and *DADI* **(b)** over SWC. About more information about these variables, their time series were also shown in Fig. S1

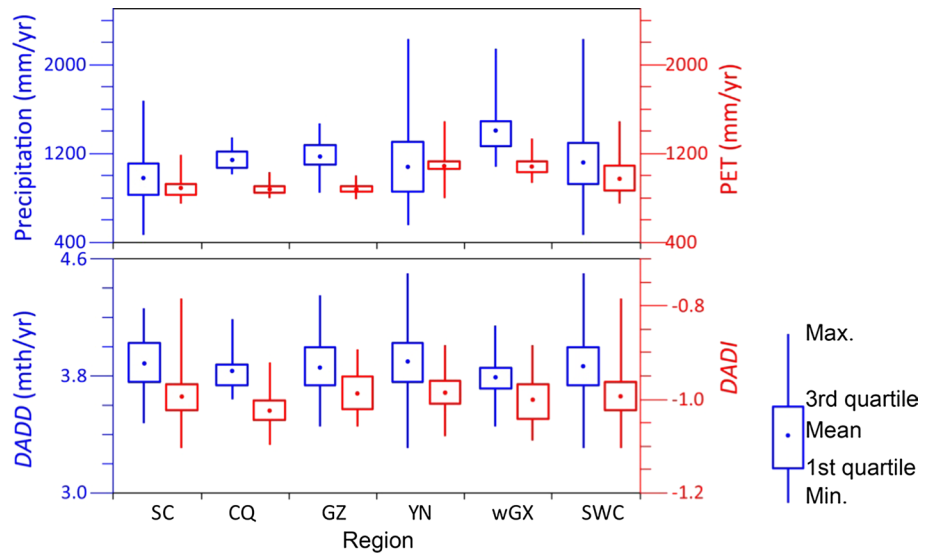


Table 1 Climatology of drought extent on 3-month scale over SWC, and their percent anomalies

Region	Climatology 1971–2012 (sites/year)	Decadal anomaly			
		1970s (%)	1980s (%)	1990s (%)	2000s+ (%)
SC	27.41	14.56	-12.87	-6.07	4.32
CQ	5.79	2.24	-9.90	-3.80	11.48
GZ	15.80	-10.48	8.47	-15.54	17.56
YN	25.07	2.33	4.39	-23.77	17.05
wGX	13.05	-1.45	-1.26	-2.20	4.84
SWC	86.83	1.49	-2.23	-10.32	11.06

climatologic drought extent, duration and intensity showed complex spatial patterns, whereas their regionally averaged values differed slightly.

3.2 Decadal anomalies of precipitation, PET and drought

Although drought variations can be influenced by a number of factors, changes in precipitation and ET (can be reflected by PET) are believed to be the most important ones. Thus, decadal variations of precipitation and PET across SWC were first analyzed relative to their mean values during 1971–2012 (Fig. 4a, b). As depicted in Fig. 4a, decadal precipitation anomalies averaged over the whole SWC were all positive from 1970s to 1990s, followed by a negative anomaly of -37.49 mm/year in the period

2000s+, which was mainly because of the most part of the study with the more and the less precipitation during the first three (Fig. 7c, f and i) and the last decades (Fig. 7l), respectively. This indicated that SWC were relative wetter (drier) before (after) 2000. Corresponding to the decadal precipitation anomalies across the whole region, the positive PET anomalies during the periods 1970s and 2000s+ implied that soil moisture tended to be drier due to more water consumption by evapotranspiration; however, the negative anomalies during the periods 1980s and 1990s represented that soil moisture had potential to be wetter due to less water consumption by ET (Fig. 4b). In addition, seen from Fig. 4a, b, precipitation and PET for each province exhibited positive decadal anomalies during 1970s, while they showed negative and positive decadal anomalies respectively for the period 2000s+. In addition, allocation of the decadal behaviors of precipitation and PET during 1980s and 1990s basically differed among these provinces.

How did drought characters, namely drought extent, duration and intensity, act in response to these precipitation and PET anomalies? For this aim, we calculated decadal anomalies of these drought characters (Table 1; Fig. 4c, d). To the coupling between decadal precipitation and PET anomalies, drought responses generally differed among regions and periods. Table 1 presented the *DADE* percent anomalies for each province and the whole SWC during each period. For SWC, SC and CQ, drought extent in 1970s and 2000s+ was higher than the long-term mean value, but lower than those in 1980s and 1990s. There were consistent percent anomalies of droughts sites during 1990s (negative) and 2000s+ (positive) in GZ, YN and wGX; while, they

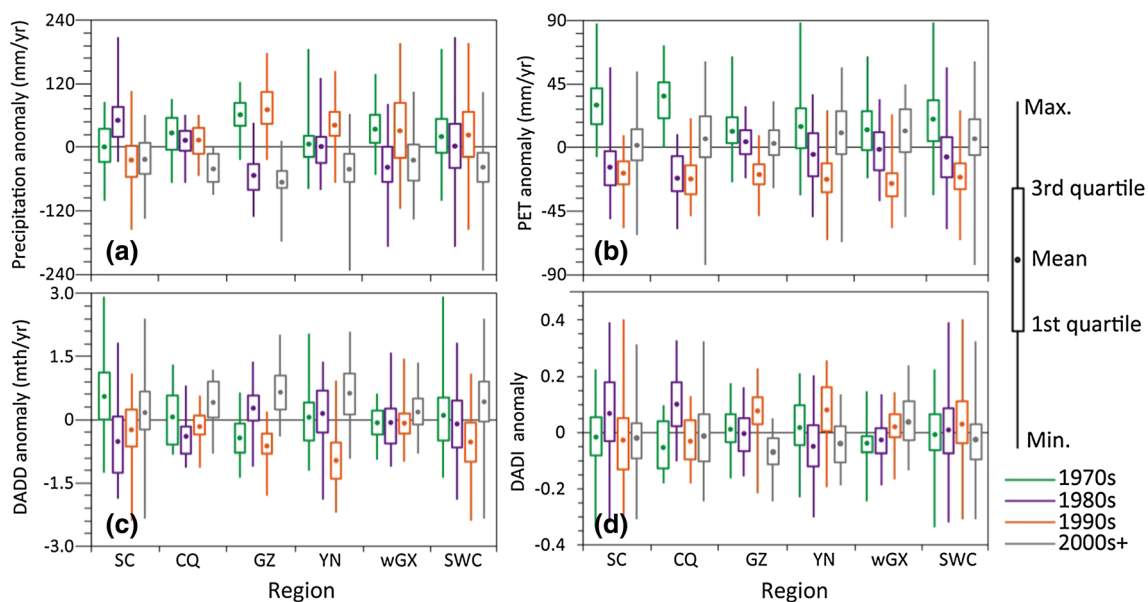


Fig. 4 Anomalies of decadal precipitation (a) and PET (b), and *DADD* (c) and *DADI* (d) across SWC. For clarity, we also showed the spatial distribution of decadal PET, *DADD* and *DADI* anomalies in Fig. S2, Fig. S3 and Fig. S4, respectively

exhibited some differences in anomalous signs in other two periods. For example, GZ, YN and wGX presented negative (positive), positive (positive) and negative (negative) anomalies in 1970s (1980s), separately. In addition, except for SC, the drought extent for each region was the largest in 2000s+, indicating that drought during this period widely happened across each province and even the whole SWC. As depicted in Fig. 4c, *DADD* anomaly for each province and the whole SWC was negative during 1990s, but positive for 2000s+. In 1970s (1980s), anomaly of *DADD* was positive (negative) for SC, CQ, and SWC, negative (positive) for GZ, positive (positive) for YN, and negative (negative) for wGX. Comparing Fig. 4c, d, it was interesting to find that *DADI* anomaly was basically opposite to those of *DADD* for a given period in some provinces of SWC. Figure 4d displayed that *DADI* anomaly for each province (excluding wGX) and SWC was negative for 2000s+, suggesting that drought intensity had intensified. For other three periods, SC consisted with CQ in *DADI* anomalies which were negative in 1970s, positive in 1980s and negative in 1990s; GZ was the same as YN with anomalies to be positive in 1970s, negative in 1980s and positive in 1990s; and wGX exhibited negative *DADI* anomalies in 1970s and 1980s, and positive ones in 1990s.

3.3 Contributions of precipitation and PET to *DADD* and *DADI* anomalies

From the above analyses, we knew that drought responses to decadal precipitation and PET anomalies differed among regions. Therefore, we hypothesized that PET also played an important role in the occurrence of drought anomaly in SWC. For testifying this hypothesis, spatial multi-linear regressions for 3-month *DADD* and *DADI* anomalies as dependent variables for each province or the entire SWC were established with independent variables of precipitation and PET anomalies to quantify precipitation and PET contributions. Also, spatial differences, such as topography (height), and latitude and longitude of sites, had been included in these regressions. Based on the least square method, regression coefficients and correlation coefficients (*R*) between the *DADD* (*DADI*) anomalies from the established regressions and those extracted from 3-month SPEI were obtained, which were shown in Table 2. It was not difficult to find that each region had a higher value than ~ 0.8 (~ 0.6) except wGX with *R* of 0.67 (0.35; Table 2); this suggested that these regressions well fitted the 3-month *DADD* (*DADI*) anomalies. As shown in Table 2, coefficients signs of decadal precipitation and PET anomalies for *DADD* were negative and positive respectively, indicating that both precipitation decreases (increases) and PET increases (decreases) would prolong (reduce) drought duration. In

contrast, positive and negative coefficients of decadal precipitation and PET anomalies for *DADI*, respectively, indicated both increases (decreases) in precipitation and decreases (increases) in PET would weaken (strengthen) drought intensity. It was not difficult to understand these findings. Based on soil water balance, precipitation increases or PET decreases would lead more water to be stored in the soil, consequently resulting in soil conditions to be unfavorable for drought evolution, and vice versa. Noteworthy, comparing precipitation and PET coefficients of *DADD* and *DADI* in each period, the larger absolute value of PET coefficient denoted that drought responses to PET anomaly were more sensitive than precipitation in SWC. Overall, from perspectives of the regressions performances (*R*) and the associated physical explanations, these regressions could relative accurately and reasonably reconstruct *DADD* (*DADI*) anomalies, which provided a potential, effective tool for quantifying contributions of decadal precipitation and PET anomalies to anomalous *DADD* (*DADI*).

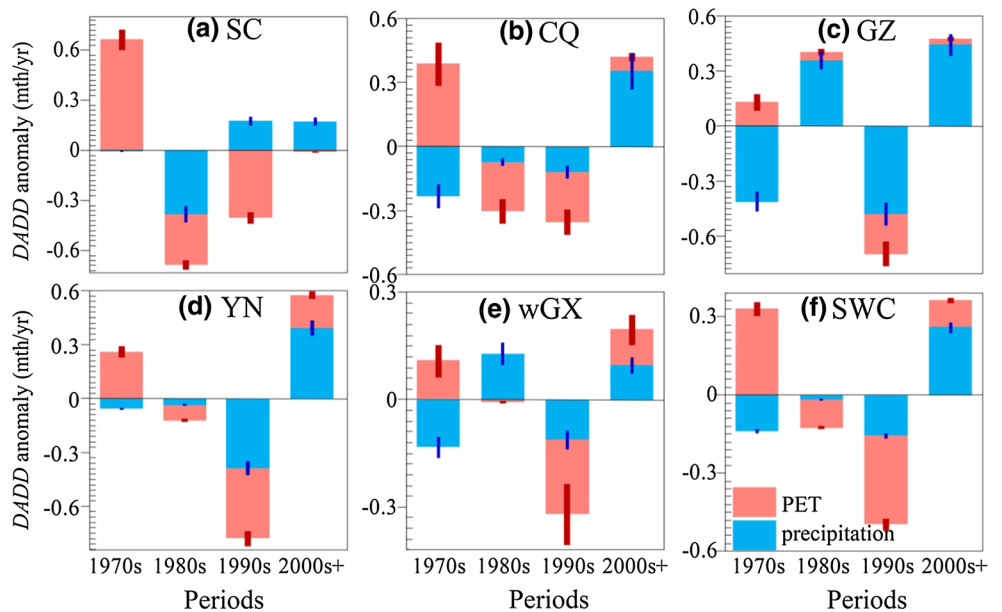
Using these multi-linear regressions parameters, we have estimated the respective contributions of decadal precipitation and PET anomalies to *DADD* and *DADI* for each period in SWC and the five provinces (Fig. 5 for *DADD* and Fig. 6 for *DADI*). Figures 5, 6 showed that anomalous PET contributions to *DADD* (*DADI*) anomalies during 1970s were all positive for each region with a range from 0.09 to 0.66 month/year (from -0.09 to -0.014), while contributions of decadal precipitation anomalies were all negative with a value between -0.41 and -0.004 (between 0.003 and 0.04). Obviously, the main causes of positive *DADD* (negative *DADI*) anomalies were positive PET variations for each region in 1970s, not including GZ where the dominant contributor was negative precipitation anomaly. For 1980s, because of complicated allocation of decadal precipitation and PET anomalies, the dominant causes of *DADD* (*DADI*) varied from region to region. Except for GZ with positive (negative) PET contribution to *DADD* (*DADI*) anomaly, SWC and other four regions all showed negative (positive) contributions ranging from -0.31 to -0.008 month/year (0.001–0.05). Meanwhile, precipitation anomalies in GZ and wGX positively (negatively) contributed to *DADD* (*DADI*), followed by other provinces and SWC showing negative (positive) contributions. Comparing contributions of PET and precipitation in 1980s, anomalies of *DADD* (*DADI*) in CQ, GZ, YN, wGX and SWC, were mainly induced by PET, precipitation, PET, precipitation, and PET, respectively; but anomalous precipitation (PET) were responsible for *DADD* (*DADI*) anomaly in SC. During 1990s, the contributions of PET and precipitation anomalies to *DADD* (*DADI*) were all negative (positive) except for precipitation in SC. In GZ, the dominant cause of *DADD* (*DADI*) anomaly was mainly because of anomalous precipitation with a contribution of

Table 2 Multi-linear regressions coefficients for 3-month drought

Coefficients	SC	CQ	GZ	YN	wGX	SWC
Duration						
Constant	0.15	-0.44	-0.36	-0.098	-0.35	-0.16
DEM	0.00001	-0.000016	-0.000015	-0.0000036	-0.000012	0.000004
LAT	-0.0023	-0.0027	-0.0043	0.00014	0.0034	-0.000086
LON	-0.0081	0.0049	-0.0045	0.00097	0.0025	0.0015
Precipitation	-0.0076*	-0.0087*	-0.0067*	-0.0095*	-0.0039*	-0.0070*
PET	0.022*	0.011*	0.011*	0.017*	0.0063*	0.017*
R^a	0.86*	0.83*	0.79*	0.88*	0.67*	0.81*
Intensity						
Constant	-0.061	0.19	0.15	0.047	0.26	0.035
DEM	-0.000001	0.000001	-0.0000007	0.00000019	-0.0000078	-0.00000083
LAT	0.00079	0.00069	-0.00097	-0.00013	-0.00047	0.00025
LON	0.00036	-0.002	-0.0012	-0.00044	-0.0023	-0.00039
Precipitation	0.0011*	0.00051*	0.00058*	0.00077*	0.000094*	0.00063*
PET	-0.0019*	-0.0024*	-0.0014*	-0.0019*	-0.0011*	-0.0018*
R	0.61*	0.69*	0.59*	0.66*	0.35*	0.58*

* Represented that the coefficient was significant at the confidence level of 5 %, while ^a was the correlation coefficients between the estimated *DADD* or *DADI* from the established regression and the derived from the 3-month SPEI. Also, we calculated the coefficients' ranges at the confidence level of 5 % (see the supplementary materials; Table S1)

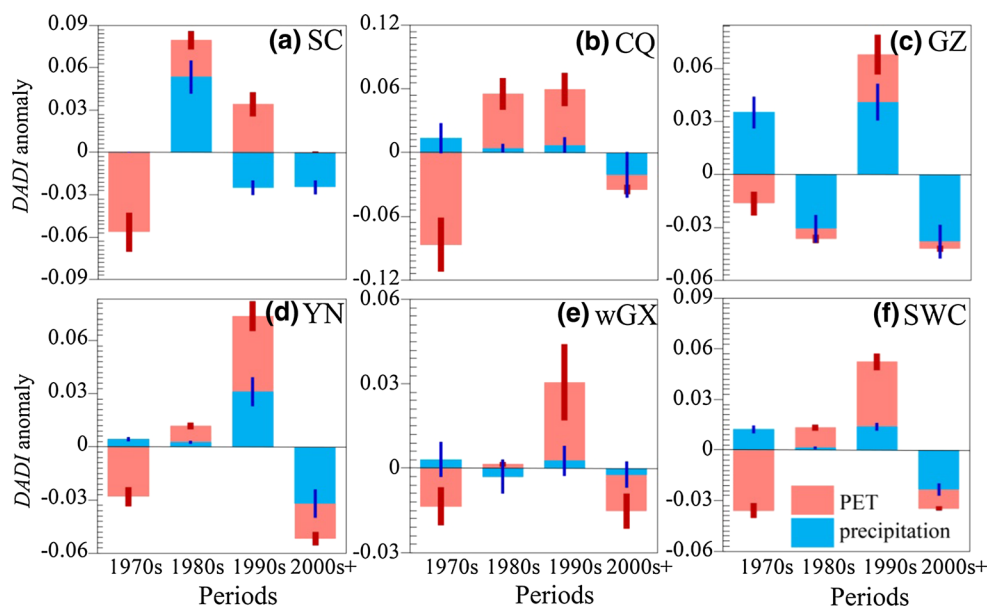
Fig. 5 Contributions of precipitation and PET to *DADD* anomalies for each period and region. Dark red and blue lines denoted the range of precipitation and PET contributions to *DADD* anomalies at the confidence level of 5 %, respectively



-0.48 month/year (0.04). Excluding GZ, SWC and other four provinces had the dominant causes of PET for *DADD* (-0.40 to -0.16 month/year) and *DADI* (0.027-0.053). In 2000s+, both precipitation and PET anomalies in each region positively (negatively) contributed to *DADD* (*DADI*). Additionally, drought intensifications of the period 2000s+

for each region (excluding wGX), including positive *DADD* and negative *DADI* anomalies, were mainly due to the greater contributions of negative precipitation anomalies. In wGX, precipitation and PET anomalies were the major contributor for positive *DADD* and negative *DADI* anomalies, respectively.

Fig. 6 Contributions of precipitation and PET to *DADI* anomalies for each period and region. Dark red and blue lines denoted the range of precipitation and PET contributions to *DADI* anomalies at the confidence level of 5 %, respectively



4 Discussions

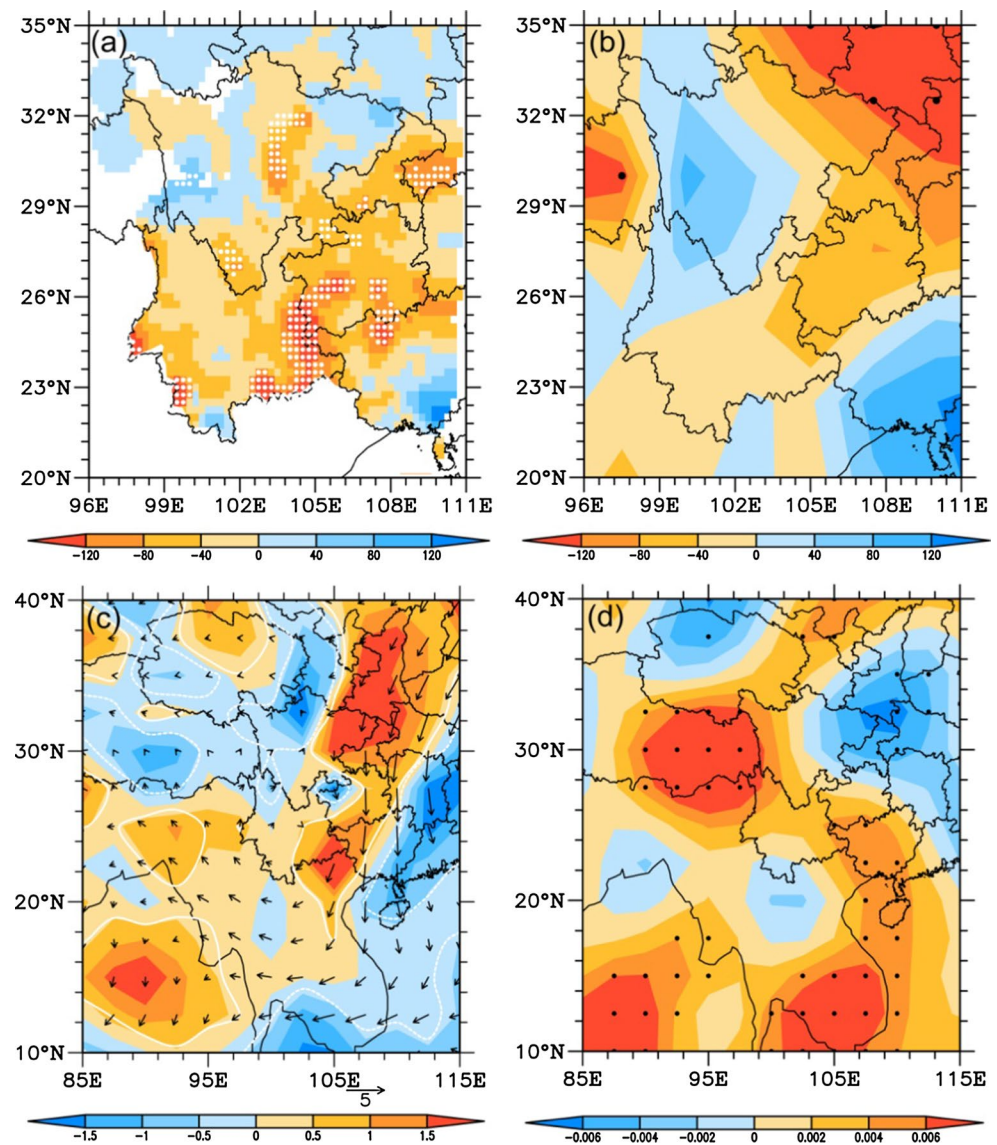
4.1 Possible causes of decadal precipitation anomalies in 2000s+

Evidences have shown that there was a decreasing trend in annual precipitation over the SWC [Liu et al. 2014; Tan et al. 2016], and our results suggested that the decreasing tendency has accelerated since 2000. As can be seen from Fig. 4a and Fig.S1a, there was no apparent trend for precipitation from 1971 to 2000, while an abrupt decrease was observed around 2000, with 2000s+ featured by prominent precipitation deficiency. This favors background for the intensification (e.g., severity, duration and extent) of the severe drought events over this study region. Most of previous studies have focused on some one single drought events (e.g., 2009/2010), whereas the investigations on the characteristics of decadal precipitation changes and the related possible causes were scarce over SWC, particularly for the precipitation deficiency in 2000s+. Therefore, we aimed to discuss the possible causes of precipitation anomalies during 2000s+ from perspective of atmospheric circulation. As is known, moisture transportation and atmospheric dynamics played fundamental roles in precipitation anomalies. Commonly, moisture convergence could increase humidity of air mass, and ascending motion usually decreases air temperature, consequently resulting in air to be saturated and then forming precipitation. Before analyzing the atmospheric dynamics with the NCEP/NCAR reanalysis data, it was necessary to compare the spatial patterns of precipitation anomalies between observational (Fig. 7a) and reanalysis datasets (Fig. 7b). Obviously, we

found that the reanalysis data could well capture the spatial characteristics of precipitation anomalies over most SWC (except for northeast SC), including the occurrence of precipitation deficiency generally in CQ, GZ and most YN, and the precipitation surplus in southeast GX and west SC. Therefore, it can be speculated that precipitation anomalies in 2000s+ were mainly caused by circulation.

During 2000s+, the moisture condition (Fig. 7c) was unfavorable for precipitation over SWC. Firstly, anomalies of the northerly moisture flux over this region oriented against the climatological flow, indicating a weakened moisture transportation from the Indian Ocean. Secondly, SWC was dominated by the moisture divergence. For example, statistical significant ($p < 0.1$) moisture anomalies could be detected at east SC, CQ, most of GZ, northwest GX and southeast YN. However, convergence anomalies were mainly located at southeast GX and northwest SC. In most regions of SWC, anomalies of moisture divergence/convergence matched well with those of precipitation. The divergence over CQ, GZ and YN corresponded to precipitation deficiency, but precipitation surplus in west SC and southeast GX could be linked to the local moisture convergence. Notably, there were also some regions where moisture conditions mismatched with precipitation anomalies, with one possible cause was that the vertical motion anomalies might reinforce or cancel out the effects of moisture divergence. For instance, despite that there was stronger moisture divergence (convergence), precipitation amount over east SC (northwest GZ) was still slightly less (more) than normal level, which was probably due to the offsetting effects of anomalous ascending (descending) motion (Fig. 7d). It was evident that over most of YN, GZ and northwest wGX, the

Fig. 7 Decadal anomalies of precipitation in observations (mm/year, **a**) and NCEP/NCAR reanalysis (mm/year, **b**), vertical integrated moisture flux (vector, 10^{-6} kg/m/s) and divergence (shaded, 10^{-6} kg/m²/s, **c**), and vertical velocity at 500 hPa (Pa/s, **d**) over SWC. Notably, positive (negative) values in **c** represented moisture divergence (convergence), while positive (negative) values in **d** denoted descending (ascending) motion. Dotted areas in **a**, **b**, **d**, and contours in **c** denoted that the anomalies were statistical significance with $p < 0.1$. Vertical integrated moisture flux and divergence, and vertical motions were calculated based on the NCEP/NCAR reanalysis dataset, while the spatial distribution of precipitation anomalies was interpolated by the bi-linear interpolation method with the 269 weather sites observations



prominent precipitation deficiency was because of moisture divergence accompanied with descending motion.

Moisture transport and atmospheric dynamic anomalies associated with SWC precipitation largely arose from external forcing of the atmosphere, such as sea surface temperature (SST), or the atmosphere internal variability. It has been noted that precipitation variability over SWC might have a link with the El Niño–Southern Oscillation (ENSO). Using composite analysis, Feng et al. (2014) found that during La Niña events, latent heating over the Maritime Continent was enhanced, which would favor downward motion over SWC through the modulation on local Hadley circulation. Apart from La Niña, Zhang et al. (2013) revealed that central Pacific El Niño events were also responsible for SWC precipitation decrease. Notably, after 1990s, central Pacific El Niño events occurred more frequently, which was favorable for decadal precipitation decrease over SWC

(Zhang et al. 2014). Wang et al. (2015b) stated that increasing trend of tropical Northwest Pacific SST also promoted decrease in SWC precipitation during autumn. Atmospheric internal variability (e.g., North Atlantic Oscillation, NAO) also had a significant impact on SWC precipitation. Negative NAO could trigger an anomalous anticyclone over subtropical Asia through Rossby wave energy propagation, thereby decreasing precipitation in SWC (Ju et al. 2011). Additionally, it is well known that SWC has complicated topography (seen in Fig. 1), e.g., Yunnan–Guizhou plateau, Sichuan basin and Qinghai–Tibetan plateau, which could lead to prominent regional climate. For example, Qinghai–Tibetan plateau could significantly influence water vapor flux (Tao et al. 1999) and atmospheric circulation via land surface processes (Wu and Zhang 1998; Wu et al. 2004; Liang et al. 2005; Zhu et al. 2007), and consequently SWC precipitation.

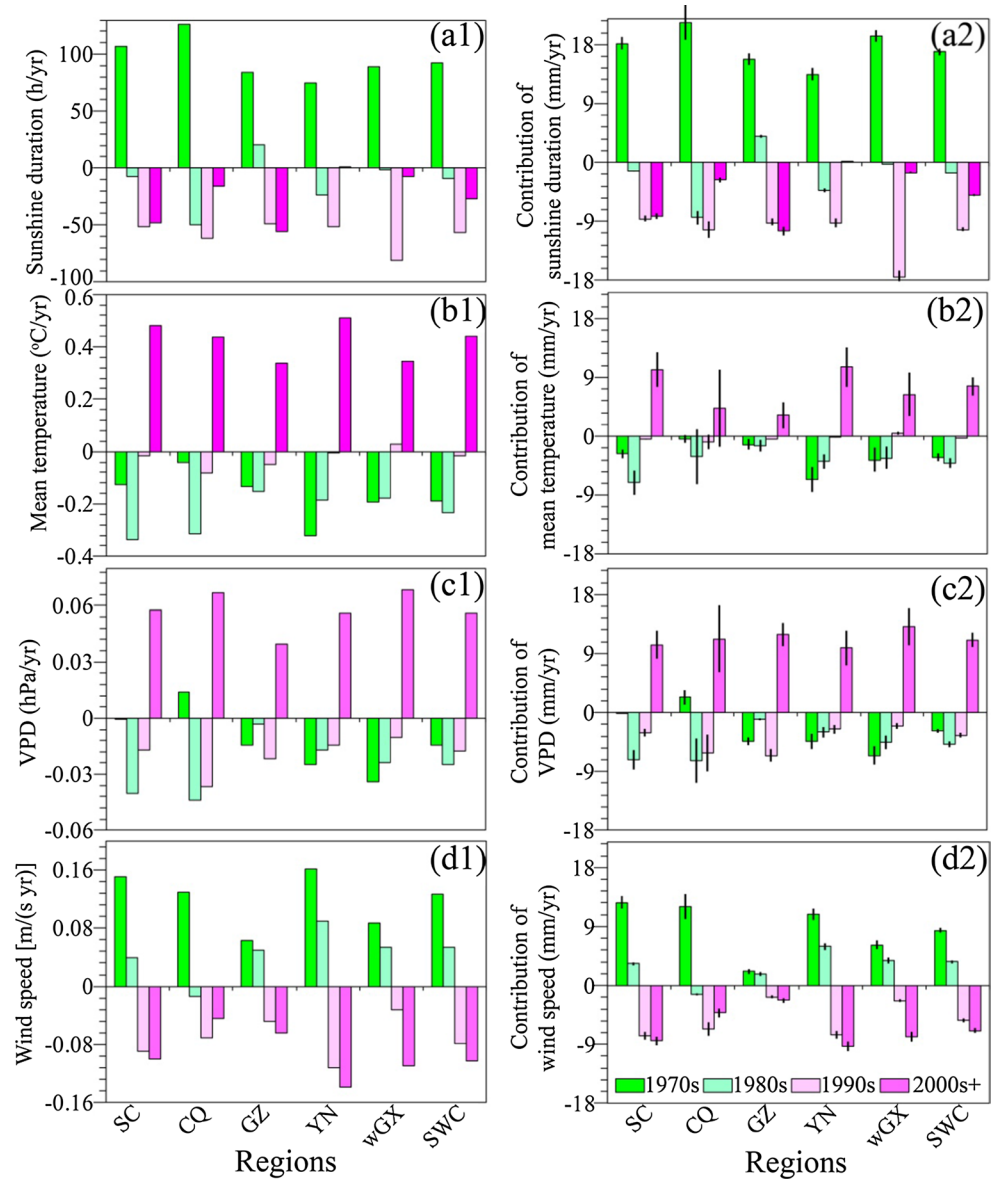
4.2 Causes of decadal PET anomalies

As climate change and human activities were exacerbating, global water balance was believed to be changing significantly, and many have already done so; whereas intensity and characteristics of such alteration might vary spatially (IPCC 2014). In the recent years, numerous studies have focused on prior and future changes in water cycle (e.g., ET and runoff/streamflow) as well as its underlying drivers on global, regional and watershed scale (Roderick and Farquhar 2002, 2004; Roderick et al. 2007; Chaplot 2007; Andréasson et al. 2004; Gosling et al. 2010; Sun et al. 2010, 2012, 2013, 2014). For instance, Roderick and Farquhar (2002) demonstrated that the large, widespread decreases in sunlight exposure due to cloud coverage and aerosol concentration increases was the major cause of the declining terrestrial evaporation over the past 50 years. Sun et al. (2010) revealed that the decreases in annual pan evaporation in Jiangxi Province of China were mainly because of the reduced daily hours of sunlight and wind speed. From the above analyses, the fact that decadal PET anomaly could impact on drought (i.e., *DADD* and *DADI*) in SWC was beyond doubt. What was more, PET contributions to drought were greater than precipitation at some time, such as in 1970s, 1980s and 1990s for SWC, suggesting that PET impacts on drought were also an indispensable, important item for explaining drought changes. Therefore, to quantify what magnitude climate change induced PET was helpful for understanding drought changes comprehensively.

Seen from the Penman–Monteith equation employed in this study, sunshine duration (can reflect net radiation), mean temperature, *VPD* and wind speed were the major determinant factors of PET. We first analyzed decadal anomalies of these climate variables during each period in each province and SWC (Fig. 8a1–d1). Generally, decadal anomalies of sunshine durations in these regions were positive in 1970s but negative during the other three periods; and moreover, comparing these anomalies during 1970s to 2000s+, there were also an obvious phenomenon of global dimming around 1980s and brightening after then in SWC, which generally coincided with the findings over the world (Wild et al. 2005, 2007; Kumari et al., 2007; Ohmura 2009; Wang et al. 2013a, b; Shen et al. 2014; Stanhill and Ahiman 2014; Rahimzadeh et al. 2015). Previous studies have pointed out that changes in sunshine duration were associated with cloud coverage, and air pollution and aerosol loading from rapid urbanization (Roderick and Farquhar 2002; Qian et al. 2007; Li et al. 2012; Yang et al. 2012b; Wang et al. 2013a, b; Kang et al. 2014; Stanhill et al. 2014). In response to continuously global warming over the past century possibly due to anthropogenic activities, such as greenhouse gases (e.g., CO₂) emissions (IPCC 2013; Xu

et al. 2015c), decadal anomalies of mean temperature in each province and SWC were basically negative in the periods of 1970s–1990s, but positive in 2000s+. Interestingly, temperature over these study areas negatively responded to sunshine duration in 1970s and 2000s+, which were seemingly contrary to our common knowledge. To address this issue, numerous researches have been carried out from a perspective of the Earth's energy budget (Philipona and Dürr, 2004; Dong et al. 2006; Wild et al. 2007, 2008; Stanhill 2011; Stanhill et al. 2013; Stanhill and Ahiman 2014; Deng et al. 2015; Longinov et al. 2014; van den Besseelaar et al. 2015), and the scholars found that temperature changes were mainly controlled by the long-wave radiation, whose variations were closely linked to clouds, water vapor, precipitation, wind speed, greenhouse gases and aerosols, and their complex interactions (Dai et al. 1997, 1999; Wild et al. 2007; Stanhill 2011; Longinov et al. 2014; Stanhill and Ahiman 2014; Lin et al. 2015). For decadal anomalies of *VPD* in all these regions, the first three and the last periods generally showed to be negative and positive, respectively, which mainly depended on synergistic variations of e_s and R_h viewed from the formula of *VPD* [= $e_s \times (1 - R_h)$]. Therefore, we also calculated their decadal anomalies for each subregion and SWC: (1) e_s : negative from 1970s to 1990s but positive in 2000s+ (Fig. S5a) in responses to the continuously increasing maximum and minimum temperatures (Shen et al. 2014; Qin et al. 2015b); and (2) R_h : generally positive and negative during the first three and the last decades, respectively (Fig. S5b), which agreed with the previous results that an abrupt decrease in R_h occurred over land areas in the last decade (Dai 2006; Simmons et al. 2010; Xie et al. 2011; Vicente-Serrano et al. 2014). During 1970s–1990s/2000s+, the positive/negative R_h anomalies might be explained from two aspects, including (a) the relative lower/higher temperature (Fig. 8b1), which indicated the lower/higher e_s (Fig. S5a), and (b) the more/less moisture supply from the main terrestrial and oceanic areas, which could be reflected by the decadal precipitation anomalies (Fig. 4a). Decadal wind speed anomalies for all the regions (excluding CQ in 1970s) appeared to be positive in 1970s and 1980s but negative in the other two periods, which were generally consistent with the previous results (Xu et al. 2006; Guo et al. 2013; Lin et al. 2013; Yang et al. 2012c). These researchers pointed out that the spatial gradient of surface global warming or cooling (e.g., land vs. ocean) might be the main cause of wind speed decreases at a regional scale through atmospheric thermal adaptation. Therefore, it was not difficult to understand that the lower/higher temperature over SWC would like to accompany with the stronger/weaker wind speed in the first/last two decades (Fig. 8b1 vs. d1). In addition, it was to be noted that anthropogenic activities, including land use/cover change (especially for urbanization) and air

Fig. 8 Decadal anomalies of the major PET driving factors **a** during 1970s to 2000s+, and their contributions to decadal PET anomalies **b** for each study region. Vertical dark line of the right panel denoted the range of driving factors' contributions to decadal PET anomalies at the confidence level of 5 %



pollution, could also influence wind speed (Klink 1999, 2002; Xu et al. 2006; Ren et al. 2008; Wang et al. 2014b). All in all, the major climatic factors (e.g., sunshine duration, mean temperature, VPD and wind speed) over SWC showed an apparent decadal changes, characterized by complex couplings among them. Despite that, the further analyses about the underlying physical mechanisms were beyond of this study scope, and thus we would like to do this in the future work.

Although the change signs of each PET driving factor were basically the same, their magnitudes varied from region to region. Using a similar method of multi-linear regression for quantifying contributions of decadal precipitation and PET anomalies to drought, we also obtained the regression coefficients of PET with *R* of higher than 0.95, which were shown in Table 3. In terms of these

coefficients, the driving factors could significantly influence PET, but their magnitudes differed. Then, through multiplying coefficient by the decadal anomaly of some one driving factor for each period in each region, we calculated their contributions to decadal PET anomalies which were displayed in Fig. 8a2–d2. In 1970s, dominant contributors for positive decadal PET anomalies in each region were mainly higher sunshine duration and stronger wind speed relative to the multi-year mean. During 1980s, the negative decadal PET anomalies in SC, CQ, wGX and SWC were mainly due to lower VPD, while higher wind speed was attributed to the positive decadal PET anomalies in GZ, and the integrated contributions of lower sunshine duration, mean temperature and VPD was responsible for the negative decadal PET anomaly in YN. For 1990s, the main contributors for decadal PET anomalies were weaker

Table 3 Multi-linear regressions coefficients for PET

Coefficients	SC	CQ	GZ	YN	wGX	SWC
Constant	-1.32	-45.62	-6.91	-18.04	-29.24	-10.79
DEM	0.00019	-0.0035	-0.00018	0.00011	0.0013	0.00027
LAT	0.00073	-0.14	-0.034	0.19	-0.22	0.065
LON	0.0096	0.47	0.074	0.12	0.31	0.081
Sunshine duration	0.17*	0.17*	0.19*	0.18*	0.22*	0.18*
Mean temperature	20.99*	9.93	9.62*	20.70*	18.65*	17.32*
VPD	179.50*	167.92*	299.81*	176.17*	191.24*	197.27*
Wind speed	84.57*	93.16*	34.52*	67.28*	71.60*	67.05*
<i>R</i>	0.97*	0.98*	0.95*	0.95*	0.98*	0.95*

* Represents that the coefficient was significant at the confidence level of 5 %. Also, we calculated the coefficients' ranges at the confidence level of 5 % (see the supplementary materials; Table S2)

wind speed in SC and YN, lower *VPD* in CQ, GZ and the whole SWC, and shorter sunshine duration in wGX. For decadal PET anomalies in 2000s+, it was very obvious that major contributors for all these regions were because of higher *VPD*. Additionally, it was noteworthy that mean temperature could have significantly impact on PET (seen from the significance level of its regression coefficient), but they were limited and smaller comparing against others' effects, which were consistent with other previous studies (Roderick and Farquhar 2002, 2004; Roderick et al. 2007; Sun et al. 2010, 2014). This implied that impacts of other climate variables (e.g., *VPD*, wind speed and sunshine duration) on PET were more important than those of temperature, and thus more attentions should be paid on these driving factors' influences for understanding PET changes comprehensively in the future researches.

4.3 Uncertainties

In spite of the SPEI model providing a useful metric of surface moisture balance, which associated with both supply and demand considerations, several factors (e.g., soil properties, elevated atmospheric CO₂, vegetation-drought interaction and human activities) ignored by this index as formulated herein, had more or less potential to impact our results. As known to all, soil moisture always closely correlated soil properties, which determined how long and how much water would be held in soil layers. Park et al. (2004) found that water-holding capacity variation could explain most local variations of soil moisture, suggesting that soil properties played an important role in monitoring droughts. Theoretically, the elevated atmospheric CO₂ were expected to directly influence plants physiological functions through declining stomatal and canopy conductance, increasing the water use efficiency of plants, and thus decreasing ET and soil moisture losses. These expectations have been extensively observed by various vegetation datasets, and further validated by numerous modeling studies over the

world during the past decades (Field et al. 1995; Betts et al. 1997, 2007; Cramer et al. 2001; Medlyn et al. 2001; Cao et al. 2010; de Boer et al. 2011; Lammertsma et al. 2011; Miglietta et al. 2011; Warren et al. 2011; Wiltshire et al. 2013; Sun et al. 2014). It was worthy noting that, however, empirical evidences for this water use efficiency effect as a large-scale control on the surface moisture budget were still highly uncertain. For instance, Domec et al. (2009) investigated loblolly pine acclimation to long-term elevated CO₂ and demonstrated that the elevated CO₂ effect on stomatal conductance manifested only during times of high soil moisture, rather than drought. Naudts et al. (2013) pointed out that no significant additional impact of the enhanced CO₂ on soil wetness was revealed in their designed numerical simulations. Based on a modified Soil and Water Assessment Tool (SWAT) model by involving the better descriptions of plant physiology effects, Sun et al. (2014) also found that the enhanced CO₂-induced stomatal conductance had a negligible effect on ET compared to climate change across the Poyang Lake Basin of China. The third factor was drought-vegetation interaction. It was well-known that vegetation under droughts was likely to dramatically alter through controlling stomatal conductance and structure [e.g., leaf area index (LAI); Ji and Peters 2003; McDowell et al. 2008; Jain et al. 2010; Sun et al. 2015]. Additionally, Anderegg et al. (2012) and Reichstein et al. (2013) reported that droughts, especially the most severe, often resulted in a higher vapor pressure gradient between leaves and atmosphere, inducing a stress on the hydraulic system of plants. As a result, high tension in the xylem can trigger embolism and partial failure of hydraulic transport in the stem, and even potentially causes vegetation mortality (Cook et al. 2007; Allen et al. 2010; Guardiola-Claramonte et al. 2011; Adams et al. 2012). In reverse, drought-induced vegetation changes or mortality would significantly influence effectual precipitation on the land surface, ET and soil moisture losses, and thus change the drought evolution (Teuling et al. 2010). Besides the potential uncertainties mentioned above,

human activities [e.g., landuse/cover change (LUCC) and water resource facilities and management] could also exert impacts on droughts to some extent (Mu et al. 2010; Qiu, 2010). Taking deforestation as an example, soil layer was likely to become thinner because of the water loss and soil erosion, which would weaken soil water capacity. Lastly, the deforestation-induced land surface hydrological balance changes potentially resulted in more drought occurrences after deforestation.

5 Conclusion

Numerous researches have pointed out that climate extreme events, particularly for drought, have frequently and intensively occurred across the world due to the exacerbating climate change. In this current study, we selected the hotspot of SWC as a study region, and analyzed decadal drought anomalies (i.e., drought extent, duration and intensity) during 1971–2012, which were extracted from the 3-month SPEI values derived from the routine meteorological observations at 269 sites. For each province and the whole SWC, droughts in 1970s and 2000s+ was basically stronger than those in 1980s and 1990s, including greater extent, longer duration and enhanced intensity, especially in 2000s+ with the strongest drought in GZ and YN. Additionally, for quantitatively evaluating decadal precipitation and PET anomalies impacts on drought in each region, we proposed spatial multi-linear regressions for 3-month *DADD* or *DADI* anomalies as dependent variable with independent variables of precipitation and PET anomalies, and heights, latitudes and longitudes of sites. For these regions, regressions coefficients of decadal precipitation and PET anomalies for *DADD* (*DADI*) variations were all negative (positive) and positive (negative), implying that precipitation decreases (increases) and PET increases (decreases) would prolong drought duration (intensity), and vice versa. Meanwhile, absolute value of PET larger than one of precipitation suggested that drought responses to PET anomalies were more sensitivity than precipitation on the decadal time scale. Comparing the contributions of decadal precipitation and PET anomalies, results showed that: except for GZ, both *DADD* and *DADI* anomalies in 1970s and 1990s were mainly because of decadal PET, and decadal precipitation anomaly in 2000s+ was the major contributor for each region; while there were obvious regional differences for the dominant contributor of *DADD* and *DADI* anomalies in 1980s.

In this study, we found that decadal PET anomalies could exert comparative or higher impacts on *DADD* and *DADI* relative to precipitation in some periods. These findings imply that PET played a critical role in drought

evolution during drought episodes, which acted to amplify drought duration and intensity. Overall, our analyses provided a comprehensive assessments of the respective influences of decadal PET and precipitation anomalies on drought (mainly including duration and intensity) changes in SWC in the last ~40 years, which would stress the need for the enough attentions for PET in the future drought researches.

Acknowledgments This work was jointly supported by the National Natural Science Foundation of China (Grant Nos. 41401016, 41375099, 41230422 and 41561124014), the Natural Science Foundation of Jiangsu Province, China (Grant Nos. BK20151525, BK20140998 and BK20160948) and the project funded by the Priority Academic Program Development (PAPD) of Jiangsu Higher Education Institutions.

References

- Abramopoulos F, Rosenzweig C, Choudhury B (1988) Improved ground hydrology calculations for global climate models (GCMs): soil water movement and evapotranspiration. *J Clim* 1:921–941
- Abramowitz M, Stegun A (1965) *Handbook of Mathematical Functions: with Formulas, Graphs, and Mathematical Tables*. Dover Publications Inc., New York
- Adams HD, Luce CH, Breshears DD, Allen CD, Weiler M, Hale VC, Smith AMS, Huxman TE (2012) Ecohydrological consequences of drought- and infestation-triggered tree die-off: insights and hypotheses. *Ecohydrology* 5(2):145–159
- Allen RG, Pereira LS, Raes D, Smith M (1998) *Crop evapotranspiration: guidelines for computing crop requirements, irrigation and drainage paper 56*. Roma, Italia
- Allen CD, Macalady AK, Chenchouni H, Bachelet D, McDowell N, Venetier M, Kitzberger T, Rigling A, Breshears DD, Hogg EH, Gonzalez P, Fensham R, Zhang Z, Castro J, Demidova N, Lim JH, Allard G, Running SW, Semerci A, Cobb N (2010) A global overview of drought and heat induced tree mortality reveals emerging climate change risks for forests. *For Ecol Manag* 259:660–684
- Anderegg WRL, Berry JA, Smith DD, Sperry JS, Anderegg LDL, Field CB (2012) The roles of hydraulic and carbon stress in a widespread climate-induced forest die-off. *Proc Natl Acad Sci USA* 109:233–237
- Andréasson J, Bergström S, Carlsson B, Graham LP, Lindström G (2004) Hydrological change—climate change impact simulations for Sweden. *Ambio* 33(4):228–234
- Barriopedro D, Gouveia CM, Trigo RM, Wang L (2012) The 2009/10 drought in China: possible causes and impacts on vegetation. *J Hydrometeorol* 13:1251–1267
- Betts RA, Cox PM, Lee SE, Woodward FI (1997) Contrasting physiological and structural vegetation feedbacks in climate change simulations. *Nature* 387:796–799
- Betts RA, Boucher O, Collins M, Cox PM, Falloon PD, Gedney N, Hemming DL, Huntingford C, Jones CD, Sexton DMH, Webb MJ (2007) Projected increase in continental runoff due to plant responses to increasing carbon dioxide. *Nature* 448(7157):1037–1041
- Cao L, Bala G, Caldeira K, Nemani R, Ban-Weiss G (2010) Importance of carbon dioxide physiological forcing to future climate change. *Proc Natl Acad Sci USA* 107:9513–9518

- Chaplot V (2007) Water and soil resources response to rising levels of atmospheric CO₂ concentration and to changes in precipitation and air temperature. *J Hydrol* 337:159–171
- Choi M, Jacobs JM, Anderson MC, Bosch DD (2013) Evaluation of drought indices via remotely sensed data with hydrological variables. *J Hydrol* 476:265–273
- Cook ER, Seager R, Cane MA, Stahle DW (2007) North American drought: reconstructions, causes, and consequences. *Earth Sci Rev* 81:93–134
- Cramer W, Bondeau A, Woodward FI, Prentice IC, Betts RA, Brovkin V, Cox Peter M, Fisher V, Foley JA, Friend AD, Kucharik C, Lomas MR, Ramankutty N, Sitch S, Smith B, White A, Young-Molling C (2001) Global response of terrestrial ecosystem structure and function to CO₂ and climate change: results from six dynamic global vegetation models. *Glob Change Biol* 7(4):357–373
- Dai A (2006) Recent climatology, variability, and trends in global surface humidity. *J Clim* 19(15):3589–3606
- Dai A (2011) Characteristics and trends in various forms of the Palmer Drought Severity Index during 1900–2008. *J Geophys Res* 116:D12115. doi:10.1029/2010JD015541
- Dai A (2013) Increasing drought under global warming in observations and models. *Nat Clim Chang* 3:52–58
- Dai A, Del Genio AD, Fung IY (1997) Clouds, precipitation, and temperature range. *Nature* 386:665–666
- Dai A, Trenberth KE, Karl TR (1999) Effects of clouds, soil moisture, precipitation and water vapor on diurnal temperature range. *J Clim* 12:2451–2473
- Dai A, Trenberth KE, Qian T (2004) A global dataset of Palmer Drought Severity Index for 1870–2002: relationship with soil moisture and effects of surface warming. *J Hydrometeorol* 5(6):1117–1130
- de Boer HJ, Lammertsma EI, Wagner-Cremer F, Dilcher DL, Wassen MJ, Dekker SC (2011) Climate forcing due to optimization of maximal leaf conductance in subtropical vegetation under rising CO₂. *Proc Natl Acad Sci USA* 108(10):4041–4046
- Deng J, Zhang Y, Qin B, Shi K (2015) Long-term changes in surface solar radiation and their effects on air temperature in the Shanghai region. *Int J Climatol* 35(12):3385–3396
- Domec JC, Palmroth S, Ward E, Maier CA, Th  r  zien M, Oren R (2009) Acclimation of leaf hydraulic conductance and stomatal conductance of *Pinus taeda* (loblolly pine) to long-term growth in elevated CO₂ (free-air CO₂ enrichment) and N-fertilization. *Plant Cell Environ* 32(11):1500–1512
- Dong X, Xi B, Minnis P (2006) Observational evidence of changes in water vapor, clouds, and radiation at the ARM SGP site. *Geophys Res Lett* 33(19):730–732
- Donohue R, McVicar T, Roderick M (2010) Assessing the ability of potential evaporation formulations to capture the dynamics in evaporative demand within a changing climate. *J Hydrol* 386:186–197
- Duan X, You W-H, Zheng J-M (2000) The drought and flood feature in Yunnan. *Plateau Meteorol* 19(1):84–90 (in Chinese with English Abstract)
- Elsner JB, Kossin JP, Jagger TH (2008) The increasing intensity of the strongest tropical cyclones. *Nature* 455:92–95
- Federal Emergency Management Agency (FEMA) (1995) National mitigation strategy: partnerships for building safer communities. Federal Emergency Management Agency, Washington, DC, p 26
- Feng L, Li T, Yu W (2014) Cause of severe droughts in Southwest China during 1951–2010. *Clim Dyn* 43:2033–2042
- Field CB, Jackson RB, Mooney HA (1995) Stomatal responses to increased CO₂: implications from the plant to the global scale. *Plant Cell Environ* 18(10):1214–1225
- Gosling SN, Bretherton D, Haines K, Arnell NW (2010) Global hydrology modelling and uncertainty: running multiple ensembles with a campus grid. *Philos Trans R Soc A* 368:4005–4021
- Gregory JM, Mitchell JFB, Brady AJ (1997) Summer drought in northern mid-latitudes in a time-dependent CO₂ climate experiment. *J Clim* 10:662–686
- Guardiola-Claramonte M, Troch PA, Breshears DD, Huxman TE, Switanek MB, Durcik M, Cobb NS (2011) Decreased streamflow in semi-arid basins following drought-induced tree die-off: a counter-intuitive and indirect climate impact on hydrology. *J Hydrol* 406:225–233
- Guo H, Xu M, Hu Q (2013) Changes in near-surface wind speed in China: 1969–2005. *Int J Climatol* 31(3):349–358
- Hobbins MT, Dai A, Roderick ML, Farquhar GD (2008) Revisiting the parameterization of potential evaporation as a driver of long-term water balance trends. *Geophys Res Lett* 35:L12403. doi:10.1029/2008GL033840
- Hu Q, Willson GD (2000) Effect of temperature anomalies on the Palmer drought severity index in the central United States. *Int J Climatol* 20:1899–1911
- Hu H-R, Mao X-L, Liang L (2009) Temporal and spatial variations of extreme precipitation events of flood season over Sichuan Basin in last 50 years. *Acta Geogr Sin* 64(3):278–288 (in Chinese with English Abstract)
- Huang Z-Y (2011) Changes of dry-wet climate in the dry season in Yunnan (1961–2007). *Adv Clim Chang Res* 2(1):49–54 (in Chinese with English Abstract)
- Huang ZP, Chen YF (2011) Hydrostatistics. China Water Power Press, Beijing p. 209 (in Chinese)
- Huang R, Cai R, Chen J, Zhou L (2006) Inter-decadal variations of drought and flooding disasters in China and their association with the East Asian climate system. *Chin J Atmos Sci* 30:730–743 (in Chinese with English Abstract)
- IPCC (2013) The physical science basis. In: Stocker TF, Qin D, Plattner G-K, Tignor M, Allen SK, Boschung J, Nauels A, Xia Y, Bex V, Midgley PM (eds.). *Climate change 2013. Contribution of working group I to the 5th assessment report of the intergovernmental panel on climate change*. Cambridge University Press, Cambridge, p. 17
- IPCC (2014) Summary for policymakers. In: Field CB, Barros, VR, Dokken DJ, Mach KJ, Mastrandrea MD, Bilir TE, Chatterjee M, Ebi KL, Estrada YO, Genova RC, Girma B, Kissel ES, Levy AN, MacCracken S, Mastrandrea PR, White LL (eds.). *Climate change 2014: impacts, adaptation, and vulnerability. part a: global and sectoral aspects. contribution of working group ii to the fifth assessment report of the intergovernmental panel on climate change*. Cambridge University Press, Cambridge, pp. 1–32
- Jain SK, Keshri R, Goswami A, Sarkar A (2010) Application of meteorological and vegetation indices for evaluation of drought impact: a case study for Rajasthan, India. *Nat Hazards* 54:643–656
- Jensen ME, Burman RD, Allen RG (eds.) (1990) *Evapotranspiration and irrigation water requirements*. ASCE manuals and reports on engineering practices no. 70. The American Society of Civil Engineers: New York, NY, p. 360
- Ji L, Peters AJ (2003) Assessing vegetation response to drought in the northern Great Plains using vegetation and drought indices. *Remote Sens Environ* 87:85–98
- Ju J, L   J, Xie G, Huang Z (2011) Studies on the influences of persistence anomalies of MJO and AO on drought appeared in Yunnan. *J Arid Meteorol* 29(4):401–406 (in Chinese with English Abstract)
- Kang P, Feng N, Wang Z, Guo Y, Wang Z, Chen Y, Zhan J, Zhan FB, Hong S (2014) Statistical properties of aerosols and

- meteorological factors in Southwest China. *J Geophys Res* 119:9914–9930
- Klink K (1999) Trends in mean monthly maximum and minimum surface wind speeds in the coterminous United States, 1961 to 1990. *Clim Res* 13(3):193–205
- Klink K (2002) Trends and interannual variability of wind speed distributions in Minnesota. *J Clim* 15(22):3311–3317
- Kogan F, Adamenko T, Guo W (2013) Global and regional drought dynamics in the climate warming era. *Remote Sens Lett* 4(4):364–372
- Kumari BP, Londhe AL, Daniel S, Jadhav DB (2007) Observational evidence of solar dimming: offsetting surface warming. *Geogr Res Lett* 34:L21810. doi:[10.1029/2007GL031133](https://doi.org/10.1029/2007GL031133)
- Lammertsma EI, de Boer HJ, Dekker SC, Dilcher DL, Lotter AF, Wagner-Cremer F (2011) Global CO₂ rise leads to reduced maximum stomatal conductance in Florida vegetation. *Proc Natl Acad Sci USA* 108(10):4035–4040
- Li Y, Xu H, Liu D (2009) Features of the extremely severe drought in the east of Southwest China and anomalies of atmospheric circulation in summer 2006. *Acta Meteorol Sin* 67(1):122–132 (in Chinese with English Abstract)
- Li Z, Feng Q, Zhang W, He Y, Wang X, Catto N, An W, Du J, Chen A, Liu L, Hu M (2012) Decreasing trend of sunshine hours and related driving forces in Southwestern China. *Theoret Appl Climatol* 109:305–321
- Li B, Su H, Chen F, Wu J, Qi J (2013) The changing characteristics of drought in China from 1982 to 2005. *Nat Hazards* 68:723–743
- Liang XY, Liu YM, Wu GX (2005) The Impact of Qinghai-Xizang Plateau uplift on Asian general circulation in spring and summer. *Plateau Meteorol* 24(6):837–845 (in Chinese with English abstract)
- Lin C, Yang K, Qin J, Fu R (2013) Observed coherent trends of surface and upper-air wind speed over China since 1960. *J Clim* 26:2891–2903
- Lin C, Yang K, Huang J, Tang W, Qin J, Niu X, Chen Y, Chen D, Lu N, Fu R (2015) Impacts of wind stilling on solar radiation variability in China. *Sci Rep* 5:15135. doi:[10.1038/srep15135](https://doi.org/10.1038/srep15135)
- Liu M, Xu X, Sun AY, Wang K, Liu W, Zhang X (2014) Is southwestern China experiencing more frequent precipitation extremes? *Environ Res Lett* 9(6):064002. doi:[10.1088/1748-9326/9/6/064002](https://doi.org/10.1088/1748-9326/9/6/064002)
- Loginov SV, Ippolitov II, Kharyutkina EV (2014) The relationship of surface air temperature, heat balance at the surface, and radiative balance at the top of atmosphere over the Asian territory of Russia using reanalysis and remote-sensing data. *Int J Remote Sens* 35(15):5878–5898
- Lu E, Luo Y, Zhang R, Wu Q, Liu L (2011) Regional atmospheric anomalies responsible for the 2009–2010 severe drought in China. *J Geophys Res* 116:D21114. doi:[10.1029/2011JD015706](https://doi.org/10.1029/2011JD015706)
- Lü J, Ju J, Ren J, Gan W (2012) The influence of the Madden-Julian Oscillation activity anomalies on Yunnan's extreme drought of 2009–2010. *Sci China (Earth Sci)* 55(1):98–112
- McDowell N, Pockman WT, Allen CD, Breshears DD, Cobb N, Kolb T, Plaut J, Sperry J, West A, Williams DG, Yezzer EA (2008) Mechanisms of plant survival and mortality during drought: why do some plants survive while others succumb to drought? *New Phytol* 178:719–739
- McKee TB, Doesken NJ, Kleist J (1993) The relationship of drought frequency and duration to time steps, preprints. In: 8th conference on applied climatology. Anaheim, CA, 17–22 January 1993, pp. 179–184
- Medlyn BE, Barton CVM, Broadmeadow MSJ, Ceulemans R, De Angelis P, Forstreuter M, Freeman M, Jackson SB, Kellomäki S, Laita E, Rey A, Roberntz P, Sigurdsson BD, Strassmeyer J, Wang K, Curtis PS, Jarvis PG (2001) Stomatal conductance of forest species after long-term exposure to elevated CO₂ concentration: a synthesis. *New Phytol* 149(2):247–264
- Miglietta F, Peressotti A, Viola R, Körner C, Amthor JS (2011) Stomatal numbers, leaf and canopy conductance, and the control of transpiration. *Proc Natl Acad Sci USA* 108(28):E275. doi:[10.1073/pnas.1105831108](https://doi.org/10.1073/pnas.1105831108)
- Min S-K, Zhang X, Zwiers FW, Hegerl GC (2011) Human contribution to more intense precipitation extremes. *Nature* 470:378–381
- Monteith JL (1973) *Principles of environmental physics*. Elsevier, New York
- Monteith JL (1976) Evaporation and surface temperature. *Q J R Meteorol Soc* 107:1–27
- Mu X, Wang F, Feng H, Zhang R, Lu X, Gao P (2010) Human impacts on severe drought in southwest region of China. *Bull Soil Water Conserv* 30(2):1–4 (in Chinese with English Abstract)
- National Climate Center (NCC) (1998) China's 1998 severe flood and climate extremes. China's Meteorological Press, Beijing, p 137
- Naudts K, Berge J, Janssens I, Nijs I, Ceulemans R (2013) Combined effects of warming and elevated CO₂ on the impact of drought in grassland species. *Plant Soil* 369(1–2):497–507
- Ohmura A (2009) Observed decadal variations in surface solar radiation and their causes. *J Geophys Res* 114:D00D05. doi:[10.1029/2008JD011290](https://doi.org/10.1029/2008JD011290)
- Palmer WC (1965) Meteorological drought. U.S. weather bureau research paper 45, U.S. Dep. of Commerce, Washington, D. C
- Park S, Feddema JJ, Egbert SL (2004) Impacts of hydrologic soil properties on drought detection with MODIS thermal data. *Remote Sens Environ* 89:53–62
- Philipona R, Dürr B (2004) Greenhouse forcing outweighs decreasing solar radiation driving rapid temperature rise over land. *Geophys Res Lett* 31:L22208. doi:[10.1029/2004GL020937](https://doi.org/10.1029/2004GL020937)
- Qian W, Zhang Z (2012) Planetary-scale and regional-scale anomaly signals for persistent drought events over Southwest China. *Chinese J Geophys* 55(5):1462–1471 (in Chinese with English Abstract)
- Qian Y, Wang W, Leung LR, Kaiser DP (2007) Variability of solar radiation under cloud-free skies in China: the role of aerosols. *Geophys Res Lett* 34:L12804. doi:[10.1029/2006GL028800](https://doi.org/10.1029/2006GL028800)
- Qian W, Shan X, Zhu Y (2011) Ranking regional drought events in China for 1960–2009. *Adv Atmos Sci* 28(2):310–321
- Qin Y, Yang D, Lei H, Xu K, Xu X (2015a) Comparative analysis of drought based on precipitation and soil moisture indices in Haihe basin of North China during the period of 1960–2010. *J Hydrol* 526:55–67
- Qin N, Wang J, Yang G, Chen X, Liang H, Zhang J (2015b) Spatial and temporal variations of extreme precipitation and temperature events for the Southwest China in 1960–2009. *Geoenviron Dis*, 2(1), doi:[10.1186/s40677-015-0014-2](https://doi.org/10.1186/s40677-015-0014-2)
- Qiu J (2010) China drought highlights future climate threats. *Nature* 465:142–143
- Rahimzadeh F, Sanchez-Lorenzo A, Hamed M, Kruk MC, Wilde M (2015) New evidence on the dimming/brightening phenomenon and decreasing diurnal temperature range in Iran (1961–2009). *Int J Climatol* 35:2065–2079
- Reichstein M, Bahn M, Ciais P, Frank D, Mahecha MD, Seneviratne S, Zscheischler J, Beer C, Buchmann N, Frank DC, Papale D, Rammig A, Smith P, Thonicke K, van der Velde M, Vicca S, Walz A, Wattenbach M (2013) Climate extremes and the carbon cycle. *Nature* 500:287–295
- Ren GY, Zhou YQ, Chu ZY, Zhou JX, Zhang AY, Guo J, Liu XF (2008) Urbanization effects on observed surface air temperature trends in north China. *J Clim* 21(6):1333–1348
- Roderick ML, Farquhar GD (2002) The cause of decreased pan evaporation over the past 50 years. *Science* 298:1410–1411

- Roderick ML, Farquhar GD (2004) Changes in Australian pan evaporation from 1970 to 2002. *Int J Climatol* 24:1077–1090
- Roderick ML, Farquhar GD, Hobbins MT (2007) On the attribution of changing pan evaporation. *Geophys Res Lett* 34:L17403. doi:10.1029/2007GL031166
- Romm J (2011) The next dust bowl. *Nature* 478:450–451
- Sheffield J, Wood EF, Roderick ML (2012) Little change in global drought over the past 60 years. *Nature* 491(7424):435–438
- Shen X, Liu B, Li G, Wu Z, Jin Y, Yu P, Zhou D (2014) Spatiotemporal change of diurnal temperature range and its relationship with sunshine duration and precipitation in China. *J Geophys Res* 119:13163–13179
- Simmons A, Willett K, Jones P, Thorne P, Dee D (2010) Low-frequency variations in surface atmospheric humidity, temperature, and precipitation: inferences from reanalyses and monthly gridded observational data sets. *J Geophys Res* 115:D01110. doi:10.1029/2009JD012442
- Stanhill G (2011) The role of water vapor and solar radiation in determining temperature changes and trends measured at Armagh, 1881–2000. *J Geophys Res* 116:D03105. doi:10.1029/2010JD014044
- Stanhill G, Ahiman O (2014) Radiative forcing and temperature change at Potsdam between 1893 and 2012. *J Geophys Res* 119:9376–9385
- Stanhill G, Rosa R, Cohen S (2013) The roles of water vapour, rainfall and solar radiation in determining air temperature change measured at Bet Dagan, Israel between 1964 and 2010. *Int J Climatol* 33(7):1772–1780
- Stanhill G, Achiman O, Rosa R, Cohen S (2014) The cause of solar dimming and brightening at the Earth's surface during the last half century: evidence from measurements of sunshine duration. *J Geophys Res* 119:10902–10911
- Stott PA, Stone DA, Allen MR (2004) Human contribution to the European heatwave of 2003. *Nature* 432(7017):610–614
- Sun SL, Zhou SQ, Song J, Shi JH, Gu RY, Ma FM (2010) Change in pan evaporation and its driving factors in Jiangxi Province. *Trans Chinese Soc Agric Eng* 26(9):59–65 (in Chinese with English Abstract)
- Sun SL, Chen HS, Ju WM, Song J, Li JJ, Ren YJ, Sun J (2012) Past and future changes of streamflow in Poyang Lake Basin, Southeastern China. *Hydrol Earth Sys Sci* 16:2005–2020
- Sun SL, Chen HS, Ju WM, Song J, Zhang H, Sun J, Fang YJ (2013) Effects of climate change on annual streamflow using climate elasticity in Poyang Lake Basin, China. *Theoret Appl Climatol* 112(1–2):169–183
- Sun SL, Chen HS, Ju WM, Yu M, Hua WJ, Yin Y (2014) On the attribution of the changing hydrological cycle in Poyang Lake Basin, China. *J Hydrol* 514:214–225
- Sun SL, Sun G, Caldwell P, McNulty S, Cohen E, Xiao J, Zhang Y (2015) Drought impacts on ecosystem functions of the U.S. National Forests and Grasslands: part II assessment results and management implications. *For Ecol Manag* 353:269–279
- Tan L, Cai Y, An Z, Cheng H, Shen C-C, Gao Y, Edwards RL (2016) Decreasing monsoon precipitation in southwest China during the last 240 years associated with the warming of tropical ocean. *Clim Dyn*. doi:10.1007/s00382-016-3171-y
- Tao SY, Chen LS, Xu XD (1999) The second theory of Tibetan Plateau Research of atmospheric scientific experiments. Meteorological Press, Beijing p. 204–214. (in Chinese)
- Teuling AJ, Seneviratne SI, Stöckli R, Reichstein M, Moors E, Ciais P, Luysaert S, van den Hurk B, Ammann C, Bernhofer C, Dellwik E, Gianelle D, Gielen B, Grünwald T, Klumpp K, Montagnani L, Moureaux C, Sottocornola M, Wohlfahrt G (2010) Contrasting response of European forest and grassland energy exchange to heatwaves. *Nat Geosci* 3(10):722–727
- Teuling AJ, van Loon AF, Seneviratne SI, Lehner I, Marc A, Heinesch B, Bernhofer C, Thomas G, Heiko P, Uwe S (2013) Evapotranspiration amplifies European summer drought. *Geophys Res Lett* 40(10):2071–2075
- Thornthwaite CW (1948) An approach toward a rational classification of climate. *Geogr Rev* 38:55–94
- Trenberth KE, Dai A, van der Schrier G, Jones PD, Barichivich J, Briffa KR, Sheffield J (2012) Global warming and changes in drought. *Nat Clim Chang* 4:17–22
- van den Besselaar EJM, Sanchez-Lorenzo A, Wild M, Klein Tank AMGK, de Laat ATJ (2015) Relationship between sunshine duration and temperature trends across Europe since the second half of the 20th century. *J Geophys Res* 120:10823–10836
- van der Schrier G, Jones PD, Briffa KR (2011) The sensitivity of the PDSI to the Thornthwaite and Penman-Monteith parameterizations for potential evapotranspiration. *J Geophys Res* 116:D03106. doi:10.1029/2010JD015001
- Vergni L, Todisco F (2011) Spatio-temporal variability of precipitation, temperature and agricultural drought indices in Central Italy. *Agric For Meteorol* 151:301–313
- Vicente-Serrano SM, Beguería S, López-Moreno J (2010) A multiscale drought index sensitive to global warming: the standardized precipitation evapotranspiration index. *J Clim* 23:1696–1718
- Vicente-Serrano SM, Azorín-Molina C, Sanchez-Lorenzo A, Morán-Tejeda E, Lorenzo-Lacruz J, Revuelto J, López-Moreno JI, Espejo F (2014) Temporal evolution of surface humidity in Spain: recent trends and possible physical mechanisms. *Clim Dyn* 42(9–10):2655–2674
- Vicente-Serrano SM, van der Schrier G, Beguería S, Azorín-Molina C, Lopez-Moreno J-I (2015) Contribution of precipitation and reference evapotranspiration to drought indices under different climates. *J Hydrol* 526:42–54
- Wang L, Chen W (2012) Characteristics of multi-timescale variabilities of the drought over last 100 years in Southwest China. *Adv Meteorol Sci Technol* 2(4):21–26 (in Chinese with English Abstract)
- Wang L, Chen W (2014) A CMIP5 multi-model projection of future temperature, precipitation, and climatological drought in China. *Int J Climatol* 34:2059–2078
- Wang SJ, Jian ST, Xin HJ (2013a) Spatio-temporal characteristics of temperature and precipitation in Sichuan Province, Southwest China, 1960–2009. *Quatern Int* 286:103–115
- Wang YW, Yang YH, Han SM, Wang QX, Zhang JH (2013b) Sunshine dimming and brightening in Chinese cities (1955–2011) was driven by air pollution rather than clouds. *Clim Res* 56:11–20
- Wang L, Chen W, Zhou W (2014a) Assessment of future drought in Southwest China based on CMIP5 multimodel projections. *Adv Atmos Sci* 31(5):1035–1050
- Wang YW, Yang YH, Zhou XY, Zhao N, Zhang JH (2014b) Air pollution is pushing wind speed into a regulator of surface solar irradiance in China. *Environ Res Lett* 10(1):123–125
- Wang L, Chen W, Zhou W, Huang G (2015a) Drought in Southwest China: a review. *Atmos Ocean Sci Lett* 8(6):339–344
- Wang L, Chen W, Zhou W, Huang G (2015b) Teleconnected influence of tropical Northwest Pacific sea surface temperature on inter-annual variability of autumn precipitation in Southwest China. *Clim Dyn* 45(9):2527–2539
- Wang L, Chen W, Zhou W, Huang G (2016) Understanding and detecting super extreme droughts in Southwest China through an integrated approach and index. *Q J R Meteorol Soc* 142(694):529–535
- Warren JM, Pötzelsberger E, Wullschleger SD, Thornton PE, Hasenauer H, Norby RJ (2011) Ecohydrologic impact of reduced stomatal conductance in forests exposed to elevated CO₂. *Ecohydrology* 4(2):196–210

- Wells N, Goddard S, Hayes MJ (2004) A self-calibrating palmer drought severity index. *J Clim* 17:2335–2351
- Wijngaard JB, Tank AMGK, Konnen GP (2003) Homogeneity of 20th century European daily temperature and precipitation series. *Int J Climatol* 23:679–692
- Wild M, Gilgen H, Roesch A, Ohmura A, Long CN, Dutton EG, Forgan B, Kallis A, Russak V, Tsvetkov A (2005) From dimming to brightening: decadal changes in solar radiation at Earth's surface. *Science* 308:847–850
- Wild M, Ohmura A, Makowski K (2007) Impact of global dimming and brightening on global warming. *Geogr Res Lett* 34:L04702. doi:[10.1029/2006GL028031](https://doi.org/10.1029/2006GL028031)
- Wild M, Grieser J, Schär C (2008) Combined surface solar brightening and increasing greenhouse effect support recent intensification of the global land-based hydrological cycle. *Geophys Res Lett* 35(17):52–58
- Wilhite D (2000) Drought as a natural hazard: concepts and definitions. In: Wilhite DA (ed) *Drought: a global assessment*. Routledge, London, pp 3–18
- Wiltshire A, Gornall J, Booth B, Dennis E, Falloon P, Kay G, McNeall D, McSweeney C, Betts R (2013) The importance of population, climate change and CO₂ plant physiological forcing in determining future global water stress. *Glob Environ Change* 23(5):1083–1097
- Wu GX, Zhang Y (1998) Tibetan Plateau forcing and the timing of the monsoon onset over South Asia and the South China Sea. *Mon Weather Rev* 26:913–927
- Wu GX, Mao JY, Duan AM, Zhang Q (2004) Recent progress in the study on the impacts of Tibetan Plateau on Asian Summer climate. *Acta Meteorol Sin* 62(5):528–540 (**in Chinese with English abstract**)
- Xie B, Zhang Q, Ying Y (2011) Trends in precipitable water and relative humidity in China: 1979–2005. *J Appl Meteorol Climatol* 50(10):1985–1994
- Xu M, Chang CP, Fu C, Robock A, Robinson D, Zhang H (2006) Steady decline of east Asian monsoon winds, 1969–2000: evidence from direct ground measurements of wind speed. *J Geophys Res Atmos* 111(D24):906–910
- Xu K, Yang D, Xu X, Lei H (2015a) Copula based drought frequency analysis considering the spatio-temporal variability in Southwest China. *J Hydrol* 527:630–640
- Xu K, Yang D, Yang H, Li Z, Qin Y, Shen Y (2015b) Spatio-temporal variation of drought in China during 1961–2012: a climatic perspective. *J Hydrol* 526:253–264
- Xu Y, Gao X, Shi Y, Zhou B (2015c) Detection and attribution analysis of annual mean temperature changes in China. *Clim Res* 63:61–71
- Yang J, Gong D, Wang W, Hu M, Mao R (2012a) Extreme drought event of 2009/2010 over southwestern China. *Meteorol Atmos Phys* 115:173–184
- Yang X, An W, Zhang W, Chang L, Wang Y (2012b) Variation of sunshine hours and related driving forces in southwestern China. *J Lanzhou Univ (Nat Sci)* 48(5):52–60 (**in Chinese with English Abstract**)
- Yang X, Li Z, Feng Q, He Y, An W, Zhang W, Cao W, Yu T, Wang Y, Theakstone WH (2012c) The decreasing wind speed in southwest China during 1969–2009, and possible causes. *Quatern Int* 263:71–84
- Yang P, Xiao Z, Yang J, Liu H (2013) Characteristics of clustering extreme drought events in China during 1961–2010. *Acta Meteorol Sin* 27(2):186–198
- Ye T, Shi P, Wang J, Liu L, Fan Y, Hu J (2012) China's drought disaster risk management: perspective of severe droughts in 2009–2010. *Int J Disaster Risk Sci* 3(2):84–97
- Yu M, Li Q, Hayes MJ, Svoboda MD, Heim RR (2014) Are droughts becoming more frequent or severe in China based on the Standardized Precipitation Evapotranspiration Index: 1951–2010? *Int J Climatol* 34:545–558
- Zhang A, Jia G (2013) Monitoring meteorological drought in semi-arid regions using multi-sensor microwave remote sensing data. *Remote Sens Environ* 134:12–23
- Zhang J, Jiang L, Feng M, Li P (2012a) Detecting effects of the recent drought on vegetation in Southwestern China. *J Resour Ecol* 3(1):43–49
- Zhang L, Xiao J, Li J, Wang K, Lei L, Guo H (2012b) The 2010 spring drought reduced primary productivity in southwestern China. *Environ Res Lett*, 7(045706), doi:[10.1088/1748-9326/7/4/045706](https://doi.org/10.1088/1748-9326/7/4/045706)
- Zhang W, Jin FF, Zhao J, Qi L, Ren H (2013) The possible influence of a nonconventional El Niño on the severe autumn drought of 2009 in Southwest China. *J Clim* 26:8392–8405
- Zhang W, Jin FF, Turner A (2014) Increasing autumn drought over southern China associated with ENSO regime shift. *Geophys Res Lett* 41:4020–4026
- Zhu YX, Ding YH, Xu HG (2007) The decadal relationship between atmospheric heat source of winter and spring snow over Tibetan plateau and rainfall in east China. *Acta Meteorol Sin* 65(6):946–958 (**in Chinese with English Abstract**)